

Topology optimization of density type for a linear elastic body by using the second derivative of a KS function with respect to von Mises stress

Wares Chancharoen · Hideyuki Azegami

Received: date / Accepted: date

Abstract This study demonstrates the use of Newton method to solve topology optimization problems of density type for linear elastic bodies to minimize the maximum von Mises stress. We use the Kreisselmeier–Steinhauser (KS) function with respect to von Mises stress as a cost function to avoid the non-differentiability of the maximum von Mises stress. For the design variable, we use a function defined in the domain of a linear elastic body with no restriction on the range and assume that a density is given by a sigmoid function of the function of design variable. The main aim of this study involves evaluating the second derivative of the KS function with respect to variation of the design variable and to propose an iterative scheme based on an H^1 Newton method as opposed to the H^1 gradient method that was presented in previous studies. The effectiveness of the scheme is demonstrated by numerical results for several linear elastic problems. The numerical results show that the speed of the proposed H^1 Newton method exceeds that of the H^1 gradient method.

Keywords Topology optimization · Stress concentration · Kreisselmeier–Steinhauser function · H^1 gradient method · H^1 Newton method

Wares Chancharoen · Hideyuki Azegami
Graduate School of Information Science, Nagoya University,
A4-2 (780) Furo-cho, Chikusa-ku, Nagoya 464-8601, Japan
E-mail: wares@az.cs.is.nagoya-u.ac.jp

Hideyuki Azegami
E-mail: azegami@i.nagoya-u.ac.jp

1 Introduction

Problems related to locating optimum layouts and shapes of holes in continua are termed as topology optimization problems (Bendsøe, 1995). In particular, when the density is selected as a design variable, the problems are termed as topology optimization problems of density type (Sigmund and Maute, 2013). This formulation is also referred as SIMP (solid isotropic material with penalization) model (Rozvany et al., 1992; Bendsøe, 1995). In linear elastic problems, mean compliance and volume are commonly used as cost functions. However, minimizing the mean compliance does not always lead to a fully stressed design. In a few instances, results from mean compliance minimization may correspond to low durability, because stress is not considered in the cost functions.

This study focuses on minimizing problems of a stress measure. Specifically, we use the maximum von Mises stress as the stress measure. When we formulate a topology optimization problem of density type to minimize the maximum von Mises stress, we encounter three difficulties that should be overcome. Two of the aforementioned difficulties are common in the topology optimization problems of density type. The first difficulty is related to the regularity of the density obtained by the finite-element method based on gradient-based methods. This is known as a checkerboard problem. The second difficulty is that the range of the density is restricted within $[0, 1]$. The set of functions with this type of a restricted range cannot correspond to a linear space. This is because when two functions possess a range of $[0, 1]$, the range of their arbitrary linear combination does not correspond to $[0, 1]$. The Fréchet derivative is defined on a Banach space that is defined as a complete normed space (the normed space is a linear

space in which a norm is defined). This restriction leads to a difficulty in which the derivative of a cost function with respect to the density is not defined at 0 and 1, because it is not possible to consider the neighborhood around 0 and 1 within $[0, 1]$. The third difficulty corresponds to the non-differentiability of the maximum von Mises stress due to locality including the singularity and jumping property.

Several remedies were proposed for the first difficulty of the irregularity. Schemes using filters or projection functions were presented since the 1990s (Diaz and Sigmund, 1995; Sigmund and Petersson, 1998; Bourdin, 2001; Guest et al., 2004). Methods using Helmholtz-type partial differential equations as a smoother of the density were presented by Lazarov and Sigmund (2011) and Kawamoto et al. (2011). A method by Kawamoto et al. (2011) involved overcoming the second difficulty of the restriction of density within $[0, 1]$ by using a non-linear polynomial function. In addition, the authors proposed a similar method and used an H^1 gradient method for topology optimization problems of density type, because the method is considered as a gradient method in a function space of H^1 class that corresponds to a Sobolev space for the functions that are differentiable and second-order Lebesgue integrable (Azegami et al., 2011). In this method, the second difficulty was overcome by using a sigmoid function with a range corresponding to $[0, 1]$. The selection of a design variable and the definition of density is shown in Section 2.

With respect to the third difficulty related to the non-differentiability of the maximum von Mises stress, several ideas were proposed. These ideas are classified into two categories: (1) methods using local stress in cost functions and (2) methods using integrations of global stress in cost functions. A typical example of (1) involves a study by Duysinx and Bendsøe (1998) that proposed an ϵ -constraint relaxation approach based on a concept developed by Cheng and Guo (1997). In their study, the vanishing of stress constraints at zero density, which is another difficulty with stress functionals in density approaches, is overcome by introducing a stress constraint function multiplied by the density. Conversely, a widely-known choice in (2) involves the use of the p -norm of von Mises stress (Le et al., 2010) and the Kreisselmeier-Steinhauser (KS) function (Kreisselmeier and Steinhauser, 1979, 1983; Yang and Chen, 1996). Moreover, mixed approaches of (1) and (2) were presented by Wang and Li (2013) and Zhang et al. (2013). They proposed the use of the p -norm of von Mises stress in the neighborhood of high local stress in the level-set formulation of shape optimization problem. In this study, we use the KS function as an objective cost function given prior experience in shape

optimization problems related to boundary variational type (Shimoda et al., 1998; Liu et al., 2015; Shintani and Azegami, 2013).

As previously observed, the basic framework for minimizing a stress measure in topology optimization problems is established. However, it was pointed out that convergence speed is significantly low. Recently, several attempts were made to examine this problem. Paris et al. (2010) presented derivations of first-order and directional second-order sensitivities for local, global, and block aggregated stress constraints. Allaire et al. (2016) introduced Hessian or second-order derivatives of cost functions, such as the mean compliance or a least square error with a target displacement, in the level-set formulation for shape optimization.

In this study, based on the approach of the H^1 gradient method to minimize problems of a stress measure by using the KS function as a cost function, we introduce the H^1 Newton method for topology optimization of density type to improve the convergence speed of the H^1 gradient method. In order to define the method, we evaluate the second derivative of the KS function with respect to the variation of the design variable. The effectiveness of the scheme is demonstrated by numerical results for several linear elastic problems.

In the following sections, we use the notation $W^{s,p}(D; \mathbb{R})$ to represent the Sobolev space for the set of functions defined in D that corresponds to a value of \mathbb{R} and is $s \in [0, \infty]$ times differentiable and $p \in [1, \infty]$ -th-order Lebesgue integrable. Furthermore, $L^p(\Omega_0; \mathbb{R}^d)$ and $H^s(\Omega_0; \mathbb{R}^d)$ are denoted by $W^{0,p}(\Omega_0; \mathbb{R}^d)$ and $W^{s,2}(\Omega_0; \mathbb{R}^d)$, respectively. With respect to a reflexive Sobolev space X , we denote its dual space by X' and the dual product of $(x, y) \in X \times X'$ by $\langle x, y \rangle$. Specifically, $f'(\mathbf{x})[\mathbf{y}]$ represents the Fréchet derivative $\langle f'(\mathbf{x}), \mathbf{y} \rangle$ of $f : X \rightarrow \mathbb{R}$ at $\mathbf{x} \in X$ with respect to an arbitrary variation $\mathbf{y} \in X$. Additionally, $f_{\mathbf{x}}(\mathbf{x}, \mathbf{y})[\mathbf{z}]$ represents the Fréchet partial derivative. The notation \forall is used as corresponding to “for all”, and $\mathbf{A} \cdot \mathbf{B}$ represents the scalar product $\sum_{(i,j) \in \{1, \dots, m\}^2} a_{ij} b_{ij}$ with respect to $\mathbf{A} = (a_{ij})_{ij}$, $\mathbf{B} = (b_{ij})_{ij} \in \mathbb{R}^{m \times m}$.

2 Problem formulation

Following a previous study (Azegami et al., 2011), we formulate a topology optimization problem of density type by using the KS function with respect to von Mises stress and a volume constraint function.

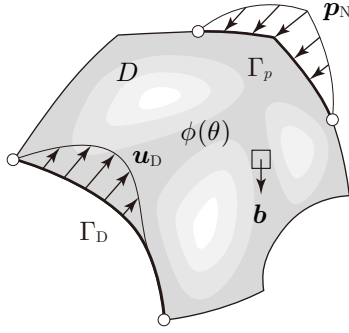


Fig. 1 Linear Elastic Problem.

2.1 Admissible set of design variable

It is assumed that D denotes a $d \in \{2, 3\}$ dimensional Lipschitz domain of a linear elastic body as shown in Fig. 1, $\theta : D \rightarrow \mathbb{R}$ is a design variable, and $\phi(\theta)$ is a density given by a sigmoid function. In the present study, we use

$$\phi(\theta) = \frac{1}{2} \tanh \theta + \frac{1}{2}. \quad (1)$$

We assume that the linear space for the design variable θ is given as

$$X = H^1(D; \mathbb{R}). \quad (2)$$

Additionally, in order to determine a Lipschitz domain with a level-set of $\phi(\theta)$, we define the admissible set of θ as

$$\mathcal{D} = X \cap W^{1,\infty}(D; \mathbb{R}). \quad (3)$$

2.2 State determination problem

With respect to a design variable $\theta \in \mathcal{D}$, we define a linear elastic problem based on the SIMP model as a state determination problem in the topology optimization problem.

We use $\mathbf{u} : D \rightarrow \mathbb{R}^d$ as the elastic displacement, $\mathbf{E}(\mathbf{u}) = \{\nabla \mathbf{u}^T + (\nabla \mathbf{u}^T)^T\}/2$ as the linear strain, $\mathbf{S}(\mathbf{u}) = \mathbf{C}\mathbf{E}(\mathbf{u})$ as the stress, and $\mathbf{C} : D \rightarrow \mathbb{R}^{d \times d \times d \times d}$ as the stiffness. It is assumed that the boundary ∂D of D consists of the Dirichlet boundary Γ_D and the Neumann boundary Γ_N , and $\mathbf{b}(\theta) : D \rightarrow \mathbb{R}^d$, $\mathbf{p}_N : \Gamma_N \rightarrow \mathbb{R}^d$ and $\mathbf{u}_D : D \rightarrow \mathbb{R}^d$ be a volume force, a traction force and a given displacement on Γ_D , respectively. Furthermore, $\boldsymbol{\nu}$ denotes the outer unit normal. We assume the power index α of $\phi(\theta)$ is a constant that exceeds 2 such that the second derivative of the cost function with respect to arbitrary variation of $\theta \in X$ is well-defined.

The fore-mentioned definitions are used to formulate the following linear elastic problem as a state determination problem.

Problem 1 (Linear elastic problem of θ type)

With respect to $\theta \in \mathcal{D}$ and given functions $\mathbf{b}(\theta)$, \mathbf{p}_N , \mathbf{u}_D and \mathbf{C} , find \mathbf{u} such that

$$\begin{aligned} -\nabla^T(\phi^\alpha(\theta) \mathbf{S}(\mathbf{u})) &= \mathbf{b}^T(\theta) \quad \text{in } D, \\ \phi^\alpha(\theta) \mathbf{S}(\mathbf{u}) \boldsymbol{\nu} &= \mathbf{p}_N \quad \text{on } \Gamma_N, \\ \mathbf{u} &= \mathbf{u}_D \quad \text{on } \Gamma_D. \end{aligned}$$

When the given functions are well-defined, $\mathbf{u} - \mathbf{u}_D$ is found uniquely in

$$U = \{\mathbf{u} \in H^1(D; \mathbb{R}^d) \mid \mathbf{u} = \mathbf{0}_{\mathbb{R}^d} \text{ on } \Gamma_D\}. \quad (4)$$

In order to determine a solution θ in \mathcal{D} by the H^1 gradient method for topology optimization problems, we need a condition that $\mathbf{u} - \mathbf{u}_D$ belongs to

$$\mathcal{S} = U \cap W^{1,2q_R}(D; \mathbb{R}^d) \quad (5)$$

for $q_R > d$.

2.3 Topology optimization problem

Using the design variable θ and the state variable \mathbf{u} , we define the cost functions for a topology optimization problem for minimizing the maximum von Mises stress.

Specifically, $\mathbf{S}(\mathbf{u})$ is denoted as $(\sigma_{ij})_{ij}$, and we define

$$\sigma(\mathbf{u}) = \sqrt{3j_2(\mathbf{u})} \quad (6)$$

where

$$\begin{aligned} j_2(\mathbf{u}) &= -(\sigma_{11}\sigma_{22} + \sigma_{11}\sigma_{33} + \sigma_{22}\sigma_{33}) \\ &\quad + \sigma_{12}^2 + \sigma_{13}^2 + \sigma_{23}^2 \end{aligned}$$

in the $d = 3$ dimensional case. The expression $\sigma(\mathbf{u})$ is used to term $\phi^\alpha(\theta) \sigma(\mathbf{u})$ as the von Mises stress.

When we employ the von Mises yield criterion for the strength of linear elastic bodies, it is necessary to minimize the maximum value of $\phi^\alpha(\theta) \sigma(\mathbf{u})$ to increase the strength. However, as mentioned in the Introduction, the maximum value of the von Mises stress is non-differentiable with respect to an arbitrary variation of $\theta \in X$. Therefore, we define the cost function by adding the KS function to the mean compliance as

$$f_0(\theta, \mathbf{u}) = f_{KS}(\theta, \mathbf{u}) + c_{MC} f_{MC}(\theta, \mathbf{u}) \quad (7)$$

where

$$f_{KS}(\theta, \mathbf{u}) = \frac{1}{p} \ln \left\{ \frac{\int_D e^{p\phi^\alpha(\theta)\sigma(\mathbf{u})/\bar{\sigma}} dx}{\int_D dx} \right\}, \quad (8)$$

$$f_{MC}(\theta, \mathbf{u}) = \int_{\Gamma_N} \mathbf{p}_N \cdot \mathbf{u} d\gamma, \quad (9)$$

$\bar{\sigma}$ denotes a positive constant to normalize $\phi^\alpha(\theta)\sigma(\mathbf{u})$, and p denotes a positive constant to control the representing property of the maximum value of $\phi^\alpha(\theta)\sigma(\mathbf{u})$ and differentiability of f_0 . Moreover, c_{MC} is a constant to control the rate of the mean compliance with respect to the KS function. As a property of the KS function, it is known that when $p \rightarrow \infty$, $f_0(\theta, \mathbf{u})$ approaches to the maximum value of $\phi^\alpha(\theta)\sigma(\mathbf{u})/\bar{\sigma}$. In this study, $\bar{\sigma}$ is selected with the maximum von Mises stress at the initial shape. The effect of changing p value is investigated in numerical examples in Section 5.

Conversely, in order to restrict the volume of the linear elastic body, we define a cost function as

$$f_1(\theta) = \int_D \phi(\theta) dx - c_1, \quad (10)$$

where c_1 denotes a positive constant such that there exists a $\theta \in D$ satisfying $f_1(\theta) < 0$. In this study, c_1 is selected as the volume of initial model.

Using these cost functions, we construct a topology optimization of linear elastic body as follows:

Problem 2 (KS function minimization problem)

For f_0 and f_1 , determine θ such that

$$\min_{(\theta, \mathbf{u}-\mathbf{u}_D) \in \mathcal{D} \times \mathcal{S}} \{f_0(\theta, \mathbf{u}) \mid f_1(\theta) \leq 0, \text{ Problem 1}\}.$$

3 Differentiations of cost functions

In this study, a solution of Problem 2 based on a Newton method is presented. In this regard, we first establish the first and the second Fréchet differentiations of the cost functions with respect to an arbitrary variation of the design variable θ that are termed as θ -derivatives and θ -Hessians of cost functions. The basic theories used in this section are summarized in the Appendix.

3.1 θ -derivatives of cost functions

Given that f_0 is a functional of the solution \mathbf{u} of Problem 2, we obtain the first θ -derivative of f_0 in the following way based on Theorem 1 in the Appendix.

We formulate the Lagrange function for f_0 as

$$\mathcal{L}_0(\theta, \mathbf{u}, \mathbf{v}_0) = f_0(\theta, \mathbf{u}) + \mathcal{L}_S(\theta, \mathbf{u}, \mathbf{v}_0). \quad (11)$$

where, \mathcal{L}_S is the Lagrange function with respect to Problem 1 defined as

$$\mathcal{L}_S(\phi, \mathbf{u}, \mathbf{v}_0) = l(\phi)(\mathbf{v}_0) - a(\phi)(\tilde{\mathbf{u}}, \mathbf{v}_0)$$

with $\tilde{\mathbf{u}} = \mathbf{u} - \mathbf{u}_D, \mathbf{v}_0 \in U$ and

$$\begin{aligned} a(\phi)(\tilde{\mathbf{u}}, \mathbf{v}_0) &= \int_{\Omega(\phi)} \phi^\alpha(\theta) \mathbf{S}(\tilde{\mathbf{u}}) \cdot \mathbf{E}(\mathbf{v}_0) dx, \\ l(\phi)(\mathbf{v}_0) &= \int_{\Omega(\phi)} \mathbf{b} \cdot \mathbf{v}_0 dx + \int_{\Gamma_p(\phi)} \mathbf{p}_N \cdot \mathbf{v}_0 d\gamma \\ &\quad - a(\phi)(\mathbf{u}_D, \mathbf{v}_0). \end{aligned}$$

If \mathbf{u} is the solution to Problem 1, then the weak form of Problem 1 is expressed as

$$\mathcal{L}_S(\theta, \mathbf{u}, \mathbf{v}_0) = 0 \quad \forall \mathbf{v}_0 \in U. \quad (12)$$

We denote $\vartheta \in X$ as the variation of θ and take the derivative of \mathcal{L}_0 with respect to the arbitrary variation $(\vartheta, \hat{\mathbf{u}}, \hat{\mathbf{v}}_0) \in X \times U^2$ of $(\theta, \mathbf{u}, \mathbf{v}_0) \in \mathcal{D} \times \mathcal{S}^2$. This results in the following expression:

$$\begin{aligned} \mathcal{L}'_0(\theta, \mathbf{u}, \mathbf{v}_0)[\vartheta, \hat{\mathbf{u}}, \hat{\mathbf{v}}_0] &= \mathcal{L}'_{0\theta}(\theta, \mathbf{u}, \mathbf{v}_0)[\vartheta] + \mathcal{L}'_{0\mathbf{u}}(\theta, \mathbf{u}, \mathbf{v}_0)[\hat{\mathbf{u}}] \\ &\quad + \mathcal{L}'_{0\mathbf{v}_0}(\theta, \mathbf{u}, \mathbf{v}_0)[\hat{\mathbf{v}}_0]. \end{aligned} \quad (13)$$

For the third term of the right-hand side in (13), we consider the following:

$$\begin{aligned} \mathcal{L}'_{0\mathbf{v}_0}(\theta, \mathbf{u}, \mathbf{v}_0)[\hat{\mathbf{v}}_0] &= \mathcal{L}'_{S\mathbf{v}_0}(\theta, \mathbf{u}, \mathbf{v}_0)[\hat{\mathbf{v}}_0] = \mathcal{L}'_S(\theta, \mathbf{u}, \hat{\mathbf{v}}_0). \end{aligned} \quad (14)$$

Subsequently, if \mathbf{u} is the solution to Problem 1, then the third term of the right-hand side in (13) corresponds to 0. Furthermore, replacing the second term of (13) with 0 results in a weak form of an adjoint problem to determine \mathbf{v}_0 . In this case, the following expression is obtained:

$$\begin{aligned} \mathcal{L}'_{0\mathbf{u}}(\theta, \mathbf{u}, \mathbf{v}_0)[\hat{\mathbf{u}}] &= \frac{1}{r(\theta, \mathbf{u})} \int_D e^{p\phi^\alpha(\theta)\sigma(\mathbf{u})/\bar{\sigma}} \phi^\alpha(\theta) \frac{\partial \sigma(\mathbf{u})}{\partial \mathbf{S}(\mathbf{u})} \cdot \frac{\mathbf{S}(\hat{\mathbf{u}})}{\bar{\sigma}} dx \\ &\quad + \int_D (-\phi^\alpha(\theta) \mathbf{S}(\hat{\mathbf{u}}) \cdot \mathbf{E}(\mathbf{v}_0) + \mathbf{b}(\theta) \cdot \hat{\mathbf{u}}) dx \\ &\quad + \int_{\Gamma_N} c_{\text{MC}} \mathbf{p}_N \cdot \hat{\mathbf{u}} d\gamma \\ &\quad + \int_{\Gamma_D} \left(\hat{\mathbf{u}} \cdot (\phi^\alpha(\theta) \mathbf{S}(\mathbf{v}_0) \boldsymbol{\nu}) \right. \\ &\quad \left. + (\mathbf{v}_0 - \mathbf{u}_D) \cdot (\phi^\alpha(\theta) \mathbf{S}(\hat{\mathbf{u}}) \boldsymbol{\nu}) \right) d\gamma, \end{aligned} \quad (15)$$

where

$$r(\theta, \mathbf{u}) = \int_D e^{p\phi^\alpha(\theta)\sigma(\mathbf{u})/\bar{\sigma}} dx. \quad (16)$$

If we assume that \mathbf{v}_0 is the solution of the following problem, then the second term of the right-hand side in (13) corresponds to 0.

Problem 3 (Adjoint problem for f_0) For $\theta \in \mathcal{D}$ and solution $\mathbf{u} \in \mathcal{S}$ of Problem 1, we determine \mathbf{v}_0 such that

$$\begin{aligned} -\nabla^T \phi^\alpha(\theta) \mathbf{S}(\mathbf{v}_0) &= -\nabla^T \Sigma(\mathbf{u}) \quad \text{in } D, \\ \phi^\alpha(\theta) \mathbf{S}(\mathbf{v}_0) \boldsymbol{\nu} &= c_{\text{MCPN}} \quad \text{on } \Gamma_N, \\ \mathbf{v}_0 &= \mathbf{0}_{\mathbb{R}^d} \quad \text{on } \Gamma_D, \end{aligned}$$

where

$$\Sigma(\mathbf{u}) = \frac{1}{\bar{\sigma} r(\theta, \mathbf{u})} \int_D e^{p\phi^\alpha(\theta)\sigma(\mathbf{u})/\bar{\sigma}} \phi^\alpha(\theta) \frac{\partial \sigma(\mathbf{u})}{\partial \mathbf{S}(\mathbf{u})} dx. \quad (17)$$

If \mathbf{u} and \mathbf{v}_0 denote the solutions of Problems 1 and 3 respectively, we obtain the θ -derivative of f_0 from the first term of the right-hand side in (13). Using the notation $\tilde{f}_0(\theta)$ to represent $f_0(\theta, \mathbf{u}(\theta))$, we obtain the following expression:

$$\tilde{f}'_0(\theta)[\vartheta] = \mathcal{L}_{0\theta}(\theta, \mathbf{u}, \mathbf{v}_0)[\vartheta] = \langle g_0, \vartheta \rangle = \int_D g_0 \vartheta dx, \quad (18)$$

where g_0 denotes the θ -gradient of f_0 that given as follows:

$$\begin{aligned} g_0 &= e^{p\phi^\alpha(\theta)\sigma(\mathbf{u})/\bar{\sigma}} (\phi^\alpha(\theta))' \frac{\sigma(\mathbf{u})}{\bar{\sigma}} \bigg/ \int_D e^{p\phi^\alpha(\theta)\sigma(\mathbf{u})/\bar{\sigma}} dx \\ &\quad + 2\mathbf{b}'(\theta) \cdot \mathbf{u} - (\phi^\alpha(\theta))' \mathbf{S}(\mathbf{u}) \cdot \mathbf{E}(\mathbf{v}_0), \end{aligned} \quad (19)$$

where

$$(\phi^\alpha(\theta))' = \alpha \phi^{\alpha-1}(\theta) \phi'(\theta) = \alpha \phi^{\alpha-1}(\theta) \frac{1}{2} \text{sech}^2 \theta. \quad (20)$$

Here, the Dirichlet conditions in Problems 1 and 3 were used.

Conversely, the θ -derivative of f_1 is obtained as

$$f'_1(\theta)[\vartheta] = \langle g_1, \vartheta \rangle = \int_D g_1 \vartheta dx, \quad (21)$$

where

$$g_1 = \phi'(\theta) = \frac{1}{2} \text{sech}^2 \theta. \quad (22)$$

3.2 θ -Hessians of cost functions

Based on the θ -derivatives of f_0 and f_1 , their θ -Hessians are obtained in the following manner.

First, we derive the θ -Hessian of f_0 based on Theorem 3 in the Appendix. Here, we assume \mathbf{b} is not a function of θ to obtain the Hessian form. Referring to (65), we define the admissible set of $(\theta, \mathbf{u} - \mathbf{u}_D)$ in Problem 2 as

$$\begin{aligned} S &= \{(\theta, \mathbf{u} - \mathbf{u}_D) \in \mathcal{D} \times \mathcal{S} \mid \\ &\quad \mathcal{L}_S(\theta, \mathbf{u}, \mathbf{v}_0) = 0 \quad \forall \mathbf{v}_0 \in U\}. \end{aligned} \quad (23)$$

Given a point $\mathbf{y}(\theta) = (\theta, \mathbf{u} - \mathbf{u}_D) \in S$, we denote the tangential plane at $\mathbf{y}(\theta)$ referring to (66) as

$$\begin{aligned} T_S(\theta, \mathbf{u}) &= \{(\vartheta, \hat{\mathbf{u}}) \in X \times U \mid \\ &\quad \mathcal{L}_{S\theta\mathbf{u}}(\theta, \mathbf{u}, \mathbf{v}_0)[\vartheta, \hat{\mathbf{u}}] = 0 \quad \forall \mathbf{v}_0 \in U\}. \end{aligned} \quad (24)$$

Using these definitions, with respect to (64), we obtain the second-order partial Fréchet derivative of \mathcal{L}_0 relative to arbitrary variations $(\vartheta_1, \hat{\mathbf{u}}_1), (\vartheta_2, \hat{\mathbf{u}}_2) \in T_S$ of $(\theta, \mathbf{u} - \mathbf{u}_D) \in S$ as

$$\begin{aligned} \mathcal{L}_{0(\theta, \mathbf{u})(\theta, \mathbf{u})}(\theta, \mathbf{u}, \mathbf{v}_0)[(\vartheta_1, \hat{\mathbf{u}}_1), (\vartheta_2, \hat{\mathbf{u}}_2)] &= \mathcal{L}_{0\theta\theta}(\theta, \mathbf{u}, \mathbf{v}_0)[\vartheta_1, \vartheta_2] + \mathcal{L}_{0\theta\mathbf{u}}(\theta, \mathbf{u}, \mathbf{v}_0)[\vartheta_1, \hat{\mathbf{u}}_2] \\ &\quad + \mathcal{L}_{0\theta\mathbf{u}}(\theta, \mathbf{u}, \mathbf{v}_0)[\vartheta_2, \hat{\mathbf{u}}_1] \\ &\quad + \mathcal{L}_{0\mathbf{u}\mathbf{u}}(\theta, \mathbf{u}, \mathbf{v}_0)[\hat{\mathbf{u}}_1, \hat{\mathbf{u}}_2]. \end{aligned} \quad (25)$$

For the first term of right-hand side of (25), we obtain the following

$$\begin{aligned} \mathcal{L}_{0\theta\theta}(\theta, \mathbf{u}, \mathbf{v}_0)[\vartheta_1, \vartheta_2] &= \int_D (\phi^\alpha(\theta))'' \left\{ \frac{\sigma(\mathbf{u})}{\bar{\sigma}} - \mathbf{S}(\mathbf{u}) \cdot \mathbf{E}(\mathbf{v}_0) \right\} \vartheta_1 \vartheta_2 dx, \end{aligned} \quad (26)$$

where

$$\begin{aligned} (\phi^\alpha(\theta))'' &= \alpha(\alpha-1) \phi^{\alpha-2}(\theta) \phi'^2(\theta) + \alpha \phi^{\alpha-1}(\theta) \phi''(\theta) \\ &= \alpha(\alpha-1) \phi^{\alpha-2}(\theta) \left(\frac{1}{2} \text{sech}^2 \theta \right)^2 \\ &\quad - \alpha \phi^{\alpha-1}(\theta) \text{sech}^2 \theta \tanh \theta. \end{aligned} \quad (27)$$

The second term of right-hand side of (25) is as follows:

$$\begin{aligned} \mathcal{L}_{0\theta\mathbf{u}}(\theta, \mathbf{u}, \mathbf{v}_0)[\vartheta_1, \hat{\mathbf{u}}_2] &= \frac{1}{r(\theta, \mathbf{u})} \int_D e^{p\phi^\alpha(\theta)\sigma(\mathbf{u})/\bar{\sigma}} (\phi^\alpha(\theta))' \\ &\quad \times \frac{\partial \sigma(\mathbf{u})}{\partial \mathbf{S}(\mathbf{u})} \cdot \frac{\mathbf{S}(\hat{\mathbf{u}}_2)}{\bar{\sigma}} \vartheta_1 dx \\ &\quad + \frac{1}{r(\theta, \mathbf{u})} \int_D e^{p\phi^\alpha(\theta)\sigma(\mathbf{u})/\bar{\sigma}} (\phi^\alpha(\theta))' p \phi^\alpha(\theta) \\ &\quad \times \frac{\sigma(\mathbf{u})}{\bar{\sigma}} \frac{\partial \sigma(\mathbf{u})}{\partial \mathbf{S}(\mathbf{u})} \cdot \frac{\mathbf{S}(\hat{\mathbf{u}}_2)}{\bar{\sigma}} \vartheta_1 dx \\ &\quad - \frac{1}{r^2(\theta, \mathbf{u})} \int_D e^{p\phi^\alpha(\theta)\sigma(\mathbf{u})/\bar{\sigma}} (\phi^\alpha(\theta))' \frac{\sigma(\mathbf{u})}{\bar{\sigma}} \vartheta_1 dx \\ &\quad \times \int_D e^{p\phi^\alpha(\theta)\sigma(\mathbf{u})/\bar{\sigma}} p \phi^\alpha(\theta) \frac{\partial \sigma(\mathbf{u})}{\partial \mathbf{S}(\mathbf{u})} \cdot \frac{\mathbf{S}(\hat{\mathbf{u}}_2)}{\bar{\sigma}} dx \\ &\quad - \int_D (\phi^\alpha(\theta))' \mathbf{S}(\hat{\mathbf{u}}_2) \cdot \mathbf{E}(\mathbf{v}_0) \vartheta_1 dx. \end{aligned} \quad (28)$$

The third term of right-hand side of (25) is obtained by replacing $\vartheta_1, \hat{\mathbf{u}}_2$ in (28) by $\vartheta_2, \hat{\mathbf{u}}_1$.

Here, given $(\vartheta_j, \hat{\mathbf{u}}_j) \in T_S$ for $j \in \{1, 2\}$, $\hat{\mathbf{u}}_j$ should satisfy the following

$$\begin{aligned} & \mathcal{L}_{S\theta\mathbf{u}}(\theta, \mathbf{u}, \mathbf{v}_0) [\vartheta, \hat{\mathbf{u}}_j] \\ &= \int_D \{ -(\phi^\alpha(\theta))' \vartheta \mathbf{S}(\mathbf{u}) - \phi^\alpha(\theta) \mathbf{S}(\hat{\mathbf{u}}_j) \} \cdot \mathbf{E}(\mathbf{v}_0) \, dx \\ &= 0 \quad \forall \mathbf{v}_0 \in U. \end{aligned} \quad (29)$$

From (29), we obtain the following expression:

$$\mathbf{S}(\hat{\mathbf{u}}_j) = -\frac{(\phi^\alpha(\theta))'}{\phi^\alpha(\theta)} \vartheta \mathbf{S}(\mathbf{u}) \quad \text{in } D. \quad (30)$$

Thus, $\hat{\mathbf{u}}_2$ and $\hat{\mathbf{u}}_1$ are substituted following (30) into (28) and for the third term of the right-hand side of (25), respectively, and it is assumed that the sum of the second and the third terms of right-hand side of (28) are negligible. This is because the stress values in the optimized density distribution converge in $\phi(\theta) \rightarrow 0$ or 1.

$$\begin{aligned} & \mathcal{L}_{0\theta\mathbf{u}}(\theta, \mathbf{u}, \mathbf{v}_0) [\vartheta_1, \hat{\mathbf{u}}_2] \\ &= \mathcal{L}_{0\theta\mathbf{u}}(\theta, \mathbf{u}, \mathbf{v}_0) [\vartheta_2, \hat{\mathbf{u}}_1] \\ &= \int_D \frac{(\phi^\alpha(\theta))'^2}{\phi^\alpha(\theta)} \left(\mathbf{S}(\mathbf{u}) \cdot \mathbf{E}(\mathbf{v}_0) \right. \\ &\quad \left. - \frac{1}{r(\theta, \mathbf{u})} e^{p\phi^\alpha(\theta)\sigma(\mathbf{u})/\bar{\sigma}} \frac{\partial \sigma(\mathbf{u})}{\partial \mathbf{S}(\mathbf{u})} \cdot \frac{\mathbf{S}(\mathbf{u})}{\bar{\sigma}} \right) \vartheta_1 \vartheta_2 \, dx. \end{aligned} \quad (31)$$

Furthermore, the fourth term of right-hand side of (25) corresponds to 0 because \mathcal{L}_0 is a linear form with respect to \mathbf{u} .

Using the fore-mentioned results and referring to (70), we obtain the θ -Hessian of f_0 as

$$\begin{aligned} & h_0(\theta, \mathbf{u}, \mathbf{v}_0) [\vartheta_1, \vartheta_2] \\ &= \mathcal{L}_{0\theta\theta}(\theta, \mathbf{u}, \mathbf{v}_0) [\vartheta_1, \vartheta_2] + \mathcal{L}_{0\theta\mathbf{u}}(\theta, \mathbf{u}, \mathbf{v}_0) [\vartheta_1, \hat{\mathbf{u}}_2] \\ &\quad + \mathcal{L}_{0\theta\mathbf{u}}(\theta, \mathbf{u}, \mathbf{v}_0) [\vartheta_2, \hat{\mathbf{u}}_1] \\ &= \int_D h_{D0} \vartheta_1 \vartheta_2 \, dx, \end{aligned} \quad (32)$$

where

$$\begin{aligned} h_{D0} &= (\phi^\alpha(\theta))'' \left\{ \frac{\sigma(\mathbf{u})}{\bar{\sigma}} - \mathbf{S}(\mathbf{u}) \cdot \mathbf{E}(\mathbf{v}_0) \right\} \\ &\quad + 2 \frac{(\phi^\alpha(\theta))'^2}{\phi^\alpha(\theta)} \left(\mathbf{S}(\mathbf{u}) \cdot \mathbf{E}(\mathbf{v}_0) \right. \\ &\quad \left. - \frac{1}{r(\theta, \mathbf{u})} e^{p\phi^\alpha(\theta)\sigma(\mathbf{u})/\bar{\sigma}} \frac{\partial \sigma(\mathbf{u})}{\partial \mathbf{S}(\mathbf{u})} \cdot \frac{\mathbf{S}(\mathbf{u})}{\bar{\sigma}} \right) \end{aligned} \quad (33)$$

In contrast, the θ -Hessian of f_1 is obtained as

$$h_1(\theta) [\vartheta_1, \vartheta_2] = \int_D h_{D1} \vartheta_1 \vartheta_2 \, dx, \quad (34)$$

where

$$h_{D1} = \phi''(\theta). \quad (35)$$

The following statements can be inferred from the results of the θ -Hessians h_0 and h_1 . In general, it is widely-known that when a Hessian in a finite dimensional vector space is a full matrix, its computational cost increases with the square of the number of design variables. However, if a Hessian is a diagonal matrix, its computational cost increases in proportion to the number of design variables. In the problem considered in this study, the θ -Hessians consist of the density, stress, and strain. Hence, they can be computed without new elements filling in the stiffness matrix of the finite element equation. Therefore, the computational cost of the θ -Hessians corresponds to the same order as that of the stiffness matrix.

4 Solutions

Using the θ -derivatives and θ -Hessians of the cost functions, we consider a scheme to solve Problem 2 based on a Newton method. This is demonstrated after discussing the H^1 gradient method alluded in the Introduction.

4.1 H^1 gradient method

Using the θ -gradients g_0 and g_1 , we apply an iterative algorithm based on the H^1 gradient method to solve Problem 2. In this section, we denote $f_0(\theta) = f_0(\theta, \mathbf{u}(\theta))$ as $f_0(\theta)$ and consider a problem that minimizes $f_0(\theta)$ under the constraints $f_1(\theta) \leq 0, \dots, f_m(\theta) \leq 0$.

For each $i \in \{0, 1, \dots, m\}$, using g_i , the H^1 gradient method involves determining the θ variation $\vartheta_{g_i} \in X$ as the solution of the following problem.

Problem 4 (H^1 gradient method of θ type) It is assumed that

$a_X : X \times X \rightarrow \mathbb{R}$ is a bounded coercive bilinear form such that there exists $\alpha_X > 0$ and $\beta_X > 0$ that satisfies

$$\begin{aligned} a_X(\vartheta, \vartheta) &\geq \alpha_X \|\vartheta\|_X^2, & \forall \vartheta \in X, \\ |a_X(\vartheta, \psi)| &\leq \beta_X \|\vartheta\|_X \|\psi\|_X, & \forall \vartheta, \psi \in X. \end{aligned}$$

For $g_i \in X'$, determine $\vartheta_{g_i} \in X$ such that

$$a_X(\vartheta_{g_i}, \psi) = -\langle g_i(\theta_k), \psi \rangle \quad \forall \psi \in X. \quad (36)$$

We confirm the unique existence of the solution ϑ_{g_i} in Problem 4 and the regularity such that ϑ_{g_i} is $W^{1,\infty}$ class from the assumption of $\mathbf{u} \in \mathcal{S}$ (Theorem 4 in Appendix). In this study, we use

$$a_X(\vartheta_{g_i}, \psi) = \int_D (\nabla \vartheta \cdot \nabla \psi + c_D \vartheta \psi) \, dx \quad (37)$$

for a_X in (36), where c_D denotes a positive constant to ensure that $a_X(\cdot, \cdot)$ corresponds to coercive bilinear form and to simultaneously control the smoothness of the solution ϑ_{g_i} . A lower c_D results in a smoother ϑ_{g_i} . Here, the strong form of Problem 4 is as follows:

$$\begin{aligned} -\Delta \vartheta_{g_i} + c_D \vartheta_{g_i} &= -g_i & \text{in } D, \\ \partial_\nu \vartheta_{g_i} &= 0 & \text{on } \partial D. \end{aligned}$$

In order to solve the problem minimizing $f_0(\theta)$ under constraints $f_i(\theta) \leq 0$ for $i \in \{0, 1, \dots, m\}$, the solutions ϑ_{g_i} of the H^1 gradient method are used, and we consider an iterative algorithm based on the following sequential quadratic approximation problem. $k \in \{0, 1, \dots\}$ denotes an iteration number.

Problem 5 (SQ approximation) For $\theta_k \in \mathcal{D}$, let g_i be given for $i \in I_A(\theta_k) = \{i \in \{1, \dots, m\} \mid f_i(\theta_k) \geq 0\}$. Additionally, c_a denotes a positive constant to control the magnitude of ϑ_{g_i} . We determine ϑ_g such that

$$q(\vartheta_g) = \min_{\vartheta \in X} \left\{ q(\vartheta) = \frac{c_a}{2} a_X(\vartheta, \vartheta) + \langle g_0, \vartheta \rangle \mid f_i(\theta_k) + \langle g_i, \vartheta \rangle \leq 0, \, i \in I_A(\theta_k) \right\}.$$

We determine the solution ϑ_g as follows. We define a Lagrange function for Problem 5 as follows:

$$\mathcal{L}_S(\vartheta, \boldsymbol{\lambda}_{k+1}) = q(\vartheta) + \sum_{i \in I_A(\theta_k)} \lambda_{i, k+1} (f_i(\theta_k) + \langle g_i, \vartheta \rangle), \quad (38)$$

where $\lambda_{i, k+1}$ denotes the Lagrange multipliers. The Karush–Kuhn–Tucker conditions at the minimum point ϑ_g are given as

$$c_a a_X(\vartheta_g, \vartheta) + \langle g_0, \vartheta \rangle + \sum_{i \in I_A(\theta_k)} \lambda_{i, k+1} \langle g_i, \vartheta \rangle = 0, \quad (39)$$

$$f_i(\theta_k) + \langle g_i, \vartheta_g \rangle \leq 0 \quad \text{for } i \in I_A(\theta_k), \quad (40)$$

$$\lambda_{i, k+1} (f_i(\theta_k) + \langle g_i, \vartheta_g \rangle) = 0 \quad \text{for } i \in I_A(\theta_k), \quad (41)$$

$$\lambda_{i, k+1} \geq 0 \quad \text{for } i \in I_A(\theta_k) \quad (42)$$

for all $\vartheta \in X$. Here, we assume

$$\vartheta_g = \vartheta_g(\boldsymbol{\lambda}_{k+1}) = \vartheta_{g_0} + \sum_{i \in I_A(\theta_k)} \lambda_{i, k+1} \vartheta_{g_i}, \quad (43)$$

where $\vartheta_{g_0}, \vartheta_{g_{i_1}}, \dots, \vartheta_{g_{i_{|I_A|}}}$ denote the solutions of the H^1 gradient method for each $g_0, g_{i_1}, \dots, g_{i_{|I_A|}}$ as

$$c_a a_X(\vartheta_{g_i}, \psi) = -\langle g_i, \psi \rangle, \quad \forall \psi \in X, \quad (44)$$

and $\boldsymbol{\lambda}_{k+1} \in \mathbb{R}^{|I_A|}$ denote unknown parameters. Subsequently, we determine that (39) holds for ϑ_g in (43) and that (40) corresponds to a linear system to determine $\boldsymbol{\lambda}_{k+1}$ when “ \leq ” is replaced by “ $=$ ” as follows:

$$\begin{aligned} (\langle g_i, \vartheta_{g_j} \rangle)_{(i,j) \in I_A^2(\theta_k)} (\lambda_{j, k+1})_{j \in I_A(\theta_k)} \\ = - (f_i(\theta_k) + \langle g_i, \vartheta_{g_0} \rangle)_{i \in I_A(\theta_k)}. \end{aligned} \quad (45)$$

Here, we use the active set method for the solution $\boldsymbol{\lambda}_{k+1}$ of (45). Thus, $\lambda_{i, k+1} = 0$ is set for $i \in I_I(\theta_k) = \{i \in I_A(\theta_k) \mid \lambda_{i, k+1} < 0\}$, $I_A(\theta_k)$ is replaced with $I_A(\theta_k) \setminus I_I(\theta_k)$, and the linear system of (40) is resolved. When $I_I(\theta_k)$ becomes \emptyset , the Karush–Kuhn–Tucker conditions are satisfied for low ϑ_g . It should be noted that when $f_i(\theta_k) = 0$ for all $i \in I_A(\theta_k)$, then $\boldsymbol{\lambda}_{k+1}$ are determined independently of the magnitude of ϑ_g .

A simple algorithm for solving a topology optimization problem is given below.

Algorithm 1 (H^1 gradient method)

1. Set θ_0 as $f_1(\theta_0) \leq 0, \dots, f_m(\theta_0) \leq 0$. Set $c_D, c_a, \epsilon_1, \dots$, and ϵ_m appropriately. Set $k = 0$.
2. Solve the state determination problem at θ_k and compute $f_0(\theta_k), f_1(\theta_k), \dots, f_m(\theta_k)$. Set $I_A(\theta_k) = \{i \in \{1, \dots, m\} \mid f_i(\theta_k) \geq -\epsilon_i\}$.
3. Solve adjoint problems at θ_k and compute $g_0, g_{i_1}, \dots, g_{i_{|I_A|}}$.
4. Solve $\vartheta_{g_0}, \vartheta_{g_{i_1}}, \dots, \vartheta_{g_{i_{|I_A|}}}$ by using (44).
5. Solve $\boldsymbol{\lambda}_{k+1}$ by using (45). When $I_I(\theta_k) \neq \emptyset$, replace $I_A(\theta_k) \setminus I_I(\theta_k)$ with $I_A(\theta_k)$, and resolve (45) until $I_I(\theta_k) = \emptyset$.
6. Compute ϑ_g using (43), set $\theta_{k+1} = \theta_k + \vartheta_g$, and compute $f_0(\theta_{k+1}), f_1(\theta_{k+1}), \dots, f_m(\theta_{k+1})$. Set $I_A(\theta_{k+1}) = \{i \in \{1, \dots, m\} \mid f_i(\theta_{k+1}) \geq -\epsilon_i\}$. (46)
7. Assess a prescribed terminal condition.
 - If “Yes,” proceed to (8).
 - If “No,” replace $k + 1$ with k and return to (3).
8. Stop the algorithm.

As a prescribed terminal condition in Step 7, it is considered that $|f_0(\theta_{k+1}) - f_0(\theta_k)| \leq \epsilon_0$ with a given $\epsilon_0 > 0$, $\|\theta_{k+1} - \theta_k\|_{W^{1,\infty}(D;\mathbb{R})} \leq \epsilon_0$ or k reaches a given number. In this study, the terminal condition using iteration number is used.

Regarding how to choose the constants c_a and c_D , the following strategy can be considered. As the first trial, $c_a = 1$ and $c_D = 1$ are recommended. As a result, when extremely fast decrease or oscillation of the objective function occurs, c_a should be replaced with a larger one in order to decrease the step size for the variation of θ . Notwithstanding this replacement, when the oscillation is not eliminated, c_D should be changed. In this case, remind that a smaller c_D increases the smoothness of variation of θ .

4.2 H^1 Newton method

When the θ -Hessians h_i of f_i for $i \in \{0, 1, \dots, m\}$ are obtained in addition to the θ -gradients g_i , an iterative algorithm based on a Newton method in X is considered. In this algorithm, the following H^1 Newton method is used as opposed to the H^1 gradient method.

Problem 6 (H^1 Newton method of θ type) For $\theta_k \in \mathcal{D}$, let the θ -gradient $g_i(\theta_k) \in X'$ and the θ -Hessian $h_i(\theta_k) \in \mathcal{L}^2(X \times X; \mathbb{R})$ of f_i be given and $a_X : X \times X \rightarrow \mathbb{R}$ correspond to a bounded coercive bilinear form to compensate for the coerciveness and the regularity of $h_i(\theta_k)$. Find $\vartheta_{gi} \in X$ such that

$$h_i(\theta_k)[\vartheta_{gi}, \psi] + a_X(\vartheta_{gi}, \psi) = -\langle g_i(\theta_k), \psi \rangle \quad \forall \psi \in X. \quad (47)$$

For the problem minimizing $f_0(\theta)$ under constraints $f_i(\theta) \leq 0$ for $i \in \{0, 1, \dots, m\}$, we replace (47) by

$$h_{\mathcal{L}}(\theta_k)[\vartheta_{gi}, \psi] + c_a a_X(\vartheta_{gi}, \psi) = -\langle g_i(\theta_k), \psi \rangle \quad \forall \psi \in X, \quad (48)$$

where

$$h_{\mathcal{L}}(\theta_k)[\vartheta_{gi}, \psi] = h_0(\theta_k)[\vartheta_{gi}, \psi] + \sum_{i \in I_A(\theta_k)} \lambda_{ik} h_i(\theta_k)[\vartheta_{gi}, \psi]. \quad (49)$$

A simple algorithm using the H^1 Newton method is given below.

Algorithm 2 (H^1 Newton method)

1. Set θ_0 as $f_1(\theta_0) \leq 0, \dots, f_m(\theta_0) \leq 0$. Set $c_D, c_a, \epsilon_1, \dots, \epsilon_m$, and k_N appropriately. Set $k = 0$.
2. Solve the state determination problem at θ_k , and compute $f_0(\theta_k), f_1(\theta_k), \dots, f_m(\theta_k)$. Set $I_A(\theta_k)$ as in (46).
3. If some $h_{i_1}, \dots, h_{i_{|I_A|}}$ is computable,
 - Solve adjoint problems at θ_k and compute g_0, g_{i_1}, \dots , and $g_{i_{|I_A|}}$.

- Solve $\vartheta_{g_0}, \vartheta_{g_{i_1}}, \dots, \vartheta_{g_{i_{|I_A|}}}$ by using (44).
 - Solve λ_{k+1} by using (45). When $I_I(\theta_k) \neq \emptyset$, replace $I_A(\theta_k) \setminus I_I(\theta_k)$ with $I_A(\theta_k)$ and resolve (45) until $I_I(\theta_k) = \emptyset$.
 - Compute ϑ_g by using (43), set $\theta_{k+1} = \theta_k + \vartheta_g$, and compute $f_0(\theta_{k+1}), f_1(\theta_{k+1}), \dots, f_m(\theta_{k+1})$. Set $I_A(\theta_k)$ as in (46).
 - Assess a prescribed terminal condition.
 - If “Yes,” proceed to (9).
 - If “No,” replace $k + 1$ with k . If $k < k_N$, return to the beginning of this step.
4. Solve adjoint problems at θ_k and compute $g_0, g_{i_1}, \dots, g_{i_{|I_A|}}$, and $h_0, h_{i_1}, \dots, h_{i_{|I_A|}}$.
 5. Solve $\vartheta_{g_0}, \vartheta_{g_{i_1}}, \dots, \vartheta_{g_{i_{|I_A|}}}$ using (48).
 6. Solve λ_{k+1} by using (45). When $I_I(\theta_k) \neq \emptyset$, replace $I_A(\theta_k) \setminus I_I(\theta_k)$ with $I_A(\theta_k)$, and resolve (45) until $I_I(\theta_k) = \emptyset$.
 7. Compute ϑ_g by using (43), set $\theta_{k+1} = \theta_k + \vartheta_g$, and compute $f_0(\theta_{k+1}), f_1(\theta_{k+1}), \dots, f_m(\theta_{k+1})$. Set $I_A(\theta_k)$ as in (46).
 8. Assess a prescribed terminal condition.
 - If “Yes,” proceed to (9).
 - If “No,” replace $k + 1$ with k and return to (4).
 9. Stop the algorithm.

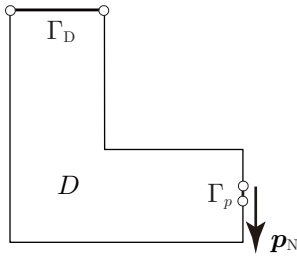
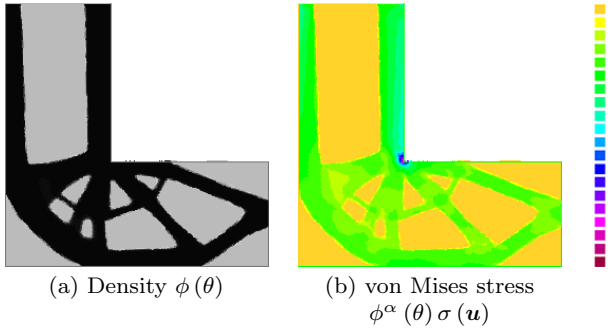
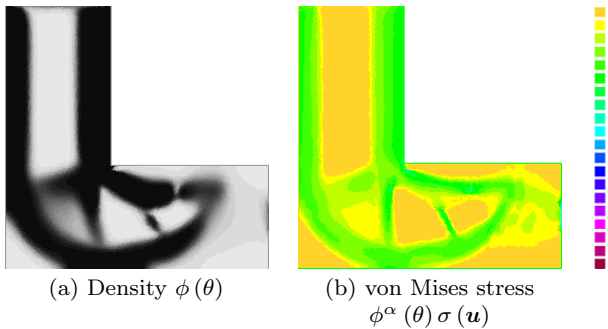
In this study, we developed a computer program to solve Problem 2 by means of a programming language by the finite element method, FreeFEM++ (Hecht, 2012). The corresponding FreeFEM++ script for the L-shaped cantilever example presented in Section 5.1 is given in detail in Appendix C.

5 Numerical examples

In order to confirm the validity of Algorithm 2 using the H^1 Newton method, we analyzed typical two-dimensional problems investigated in several studies using the developed computer programs. In these studies, we set $c_{MC} = 1$ in (7) and $k_N = 7$ in Algorithm 2. Second order triangular elements were used in the following finite element analyses. Furthermore, the function of adaptive mesh in FreeFEM++ was used with an error level for the mesh adaptation: $errelas = 0.05$.

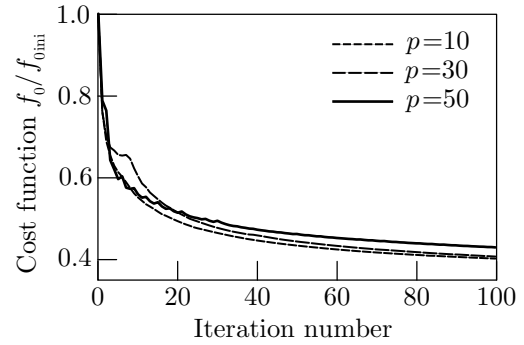
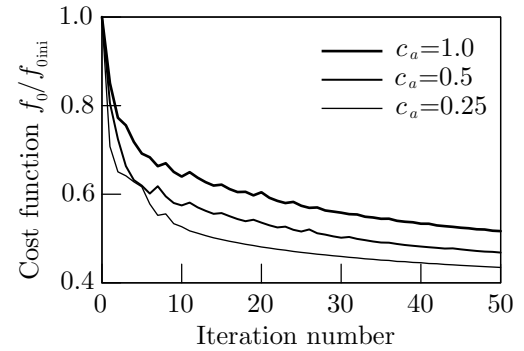
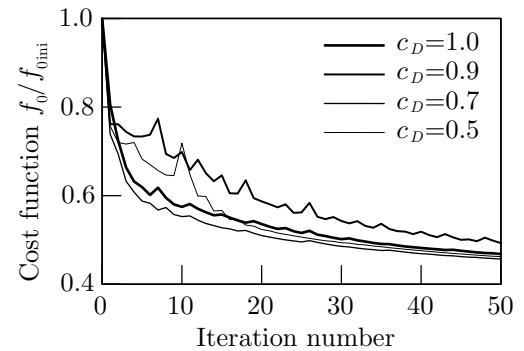
5.1 L-shaped cantilever

Figure 2 shows the geometry of a two-dimensional L-shaped cantilever assumed as the linear elastic problem in Problem 1. The height of D is 20 m. We used $\mathbf{p}_N = (0, 1)^T$ N on the non-homogeneous Neumann boundary Γ_p with a length of 0.02 m and Young’s modulus and Poisson’s ratio corresponding to 210 MPa and


Fig. 2 L-shaped cantilever problem.

Fig. 3 Result of the mean compliance f_{MC} minimization (color bar: [0, 11] MPa).

Fig. 4 Result of the KS function f_{KS} minimization (color bar: [0, 9] MPa).

0.3, respectively. Additionally, we assumed $\theta = 0$ in D at the initial model. Hence, when c_1 is selected as the volume of initial model in (10), the volume ratio $c_1 / \int_D dx$ was assumed as 0.5. Figure 3 shows the result of the mean compliance f_{MC} minimization as a reference. The result shows that the stress concentration on the re-entrant corner does not exist. Meanwhile, the result of only the KS function f_{KS} minimization ($c_{MC} = 0$ in (7)) is shown in Fig. 4. From the result, it is considered that the mean compliance is needed in order to maintain a frame of mechanical structure.

Figure 5 shows the iteration histories of f_0/f_{0ini} (f_{0ini} denotes the initial value of f_0) with varying values of p using the H^1 gradient method. In these analyses, $c_a = 0.5$ and $c_D = 0.7$ were used. These respective value of c_a and c_D were selected in the following way. We


Fig. 5 L-shaped cantilever: Iteration history of cost function f_0 in cases changing p by the H^1 gradient method.

Fig. 6 L-shaped cantilever: Iteration history of changing c_a with fixed $c_D = 0.7$ by the H^1 gradient method.

Fig. 7 L-shaped cantilever: Iteration history of changing c_D with fixed $c_a = 0.5$ by the H^1 gradient method.

made trial analyses with $c_a=1.0, 0.5$ and 0.25 and $c_D=1.0, 0.9, 0.7$ and 0.5 until $k = 50$ iterations. The results of the trial analyses are shown in Figs. 6 and 7. In view of these results, we chose $c_a = 0.5$ and $c_D = 0.7$ because they constitute to a faster and more stable convergence. The iteration histories of the maximum nodal value of von Mises stress $\phi^\alpha(\theta)\sigma(\mathbf{u})$ and $\bar{\sigma}f_{KS}(\theta, \mathbf{u})$ are shown in Fig. 8 with respect to the three cases of p . The maximum nodal value of von Mises stress is not reliable at a singular point in the finite element analysis because we can demonstrate that the stress at a concave corner point is theoretically infinite and that the nodal value

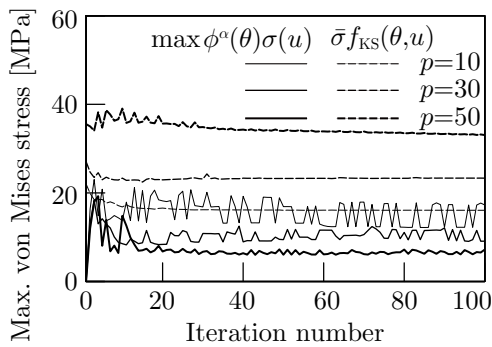


Fig. 8 L-shaped cantilever: Iteration history of the maximum nodal value of von Mises stress $\phi^\alpha(\theta)\sigma(\mathbf{u})$ and $\bar{\sigma}f_{KS}(\theta, \mathbf{u})$ in cases involving changes in p by the H^1 gradient method.

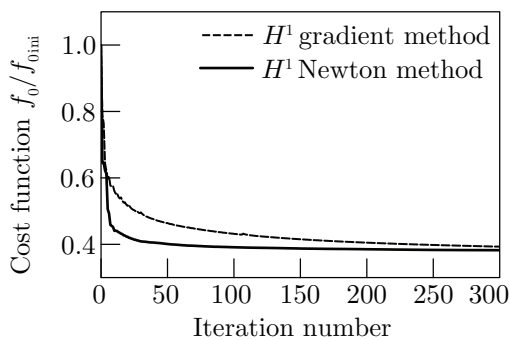


Fig. 9 L-shaped cantilever: Iteration history of the cost function f_0 for a comparison between H^1 gradient method and the H^1 Newton method when $p = 50$.

of the stress by the finite element method is affected by the mesh. Although its values are not reliable, we confirm the tendency of decreasing them at the initial stage. In contrast, $\bar{\sigma}f_{KS}(\theta, \mathbf{u})$ exhibits similar values to the maximum nodal values of von Mises stress and decreases monotonically. Based on the observation, in this study, $p=50$ was used for the L-shaped cantilever problem as the maximum value with which the feasibility was checked.

Figure 9 shows the comparison between the iteration histories of f_0/f_{0ini} by the H^1 gradient method and the H^1 Newton method while using $p=50$. The value of f_0/f_{0ini} by the H^1 gradient method at 600th iteration corresponds to 0.376 and 0.385 at 200th iteration by the H^1 Newton method. The number of nodes correspond to 1550 at 600th in the H^1 gradient method and 1030 at 200th in the H^1 Newton method. The computational times correspond to 173 h to the 600th iteration (0.29 h/iteration) and 46 h to the 200th iteration (0.23 h/iteration). The results indicate that the H^1 Newton method significantly converges faster than the H^1 gradient method. The density and the von Mises stress distributions obtained by the H^1 gradient method and the H^1 Newton method are illustrated in Figs. 10 and 11,

respectively. Figure 12 shows the mesh of final model by the H^1 Newton method. From the results, it is observed that the H^1 Newton method converges significantly faster when compared. From the results, it is observed that the stress concentrations around the re-entrant corner were relieved in both cases as opposed to the result of mean compliance minimization and that the optimized topology was approximately determined by the H^1 Newton method at 200th loop of iterations while that by the H^1 gradient method was approximately determined at the 600th iteration. The computational cost per an iteration decreased to 20%. As theoretically expected, the Newton method displays the property of quadratic convergence, and the superiority of the H^1 Newton method in terms of convergence speed was confirmed from these results.

5.2 Portal frame

Moreover, we applied the proposed method to a portal frame problem as shown in Fig. 13. The material constants and the initial value of $\theta = 0$ were the same as those of the L-shaped cantilever problem. We used $\mathbf{p}_N = (0, 1)^T$ N on the non-homogeneous Neumann boundary Γ_p with a length of 0.1 m. The height and length correspond to 60 m and 120 m, respectively. We performed a few preliminary analyses by changing the p value and selected $p = 10$ by the same manner in the L-shaped cantilever problem. From the analyses, $c_a = 1$ and $c_D = 0.7$ were selected to decrease speed of calculation and refrain the oscillation of convergence. Figure 14 shows a comparison between the iteration histories of f_0/f_{0ini} by the H^1 gradient method and the H^1 Newton method. Beyond the limit of horizontal axis of Fig. 14, the values of f_0/f_{0ini} were 0.541 by the H^1 gradient method at the 600th iteration and 0.505 by the H^1 Newton method at the 400th iteration. The number of nodes corresponded to 1189 at the 600th iteration in the H^1 gradient method and 760 at the 400th iteration in the H^1 Newton method. The computational times corresponded to 32 h to the 600th iteration (0.0533 h/iteration) and 9 h to the 400th iteration (0.0225 h/iteration). Figures 15 and 16 illustrate the density and the von Mises stress distributions obtained by the H^1 gradient method and the H^1 Newton method, respectively. Figure 17 shows the mesh of final model by the H^1 Newton method. From the results, it is observed that the H^1 Newton method converges significantly faster when compared to the H^1 gradient method. The computational cost per an iteration decreased to 57%. Moreover, with respect to Fig. 16, it is observed that the use of the H^1 Newton method significantly removes the stress concentration at the re-

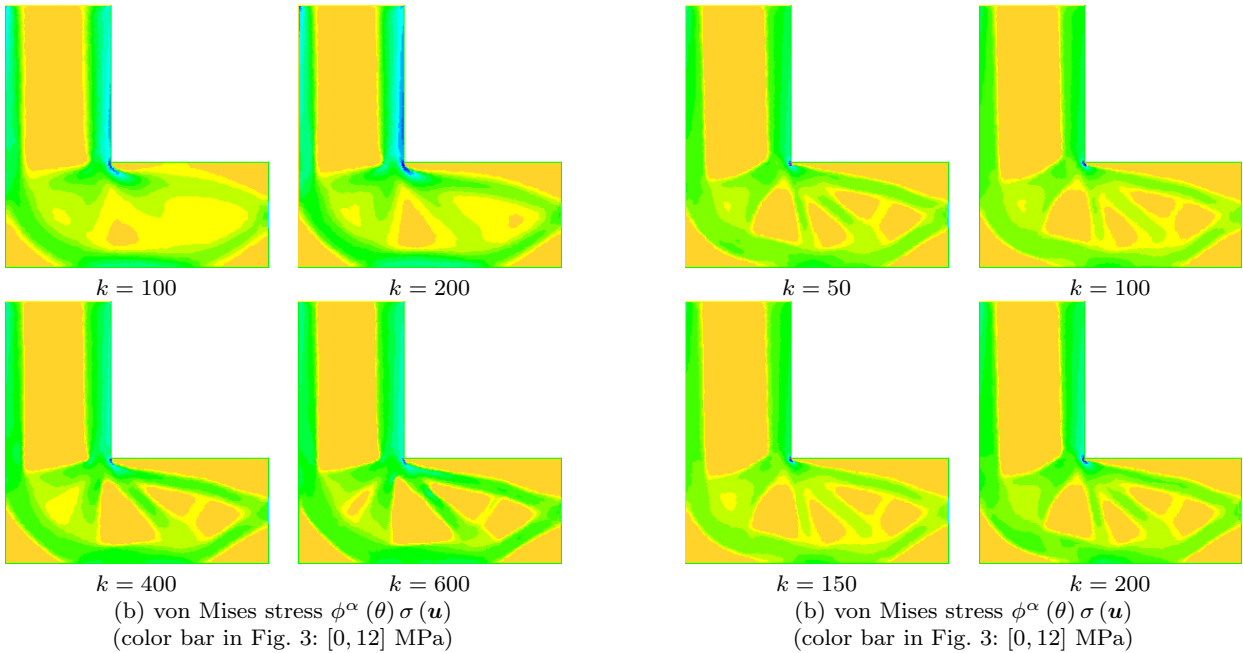
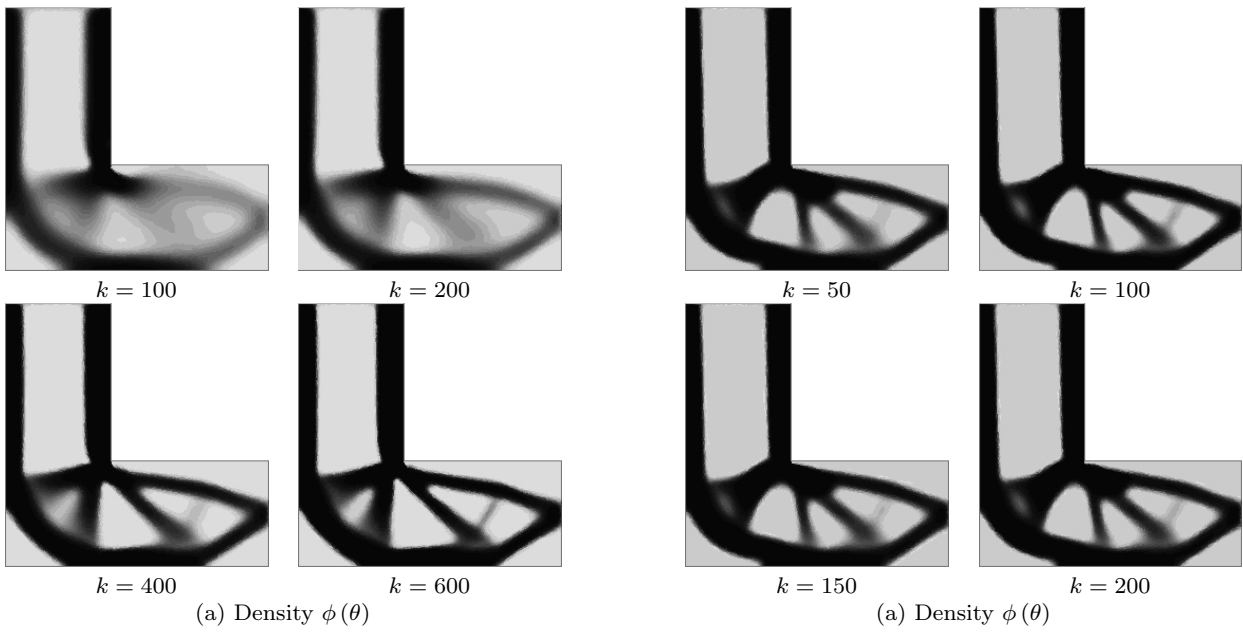


Fig. 10 L-shaped cantilever: Results of the H^1 gradient method.

Fig. 11 L-shaped cantilever: Results of the H^1 Newton method.

entrant corners by focusing attention on the difference of the color bar scales. The results of the L-shaped cantilever and the portal frame are compared, and it appears that the improvement of convergence property by the H^1 Newton method from the H^1 gradient method depends on the boundary conditions of linear elastic problems.

5.3 Comparison with literature

The problems of L-shaped cantilever and portal frame are used as benchmarks to check the validity of the newly proposed methods. Here, we compare the results of the study to those obtained by extant studies.

The L-shaped cantilever problem was used in the numerical analyses by Le et al. (2010), Bruggi and Duysinx (2012), and Holmberg et al. (2013) to check the performances of their methods although the locations of the external force \mathbf{p}_N are slightly different.

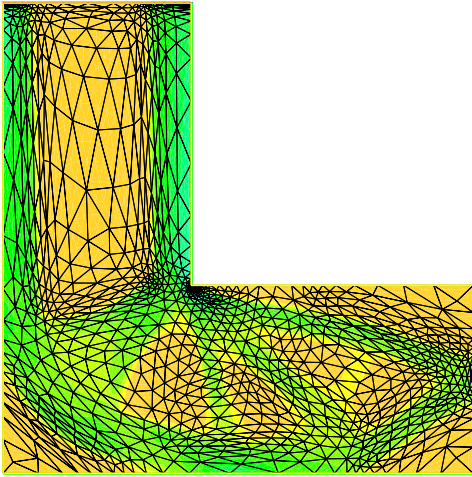


Fig. 12 Mesh of L-shaped cantilever: $k = 200$ by the H^1 Newton method.

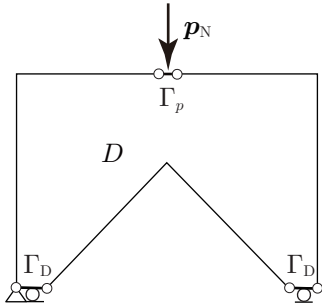


Fig. 13 Portal frame problem.

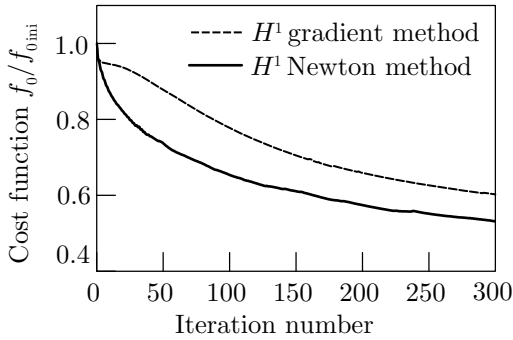


Fig. 14 Portal frame: Iteration history of the cost function f_0 for a comparison between the H^1 gradient method and the H^1 Newton method when $p = 10$.

The results illustrated in Bruggi and Duysinx (2012) use the same position that corresponds to the center of right hand edge with the current analysis. In the analyses, they select the weight as the objective cost function and constraints by using the mean compliance and/or the product of penalized density and the equivalent Drucker-Prager local stress measure. A comparison of the results in Figs. 10 and 11 with the results by Bruggi and Duysinx (2012) confirms that the topol-

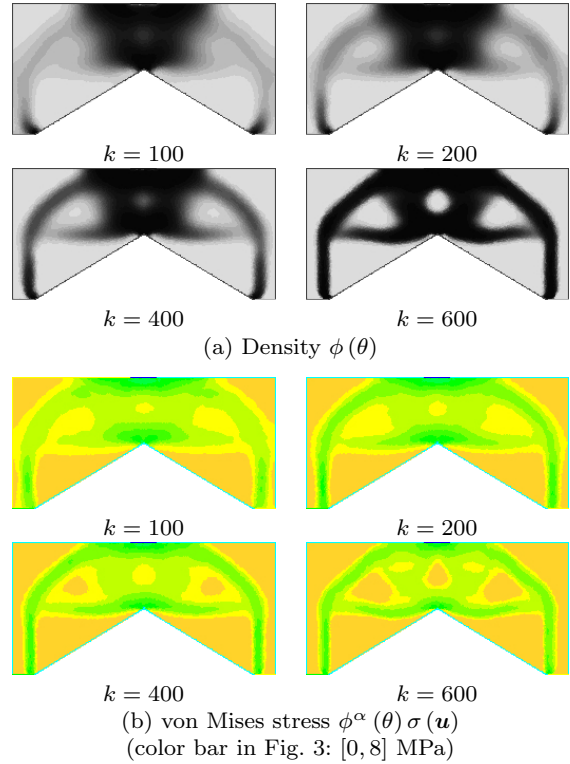


Fig. 15 Portal frame: Results of the H^1 gradient method.

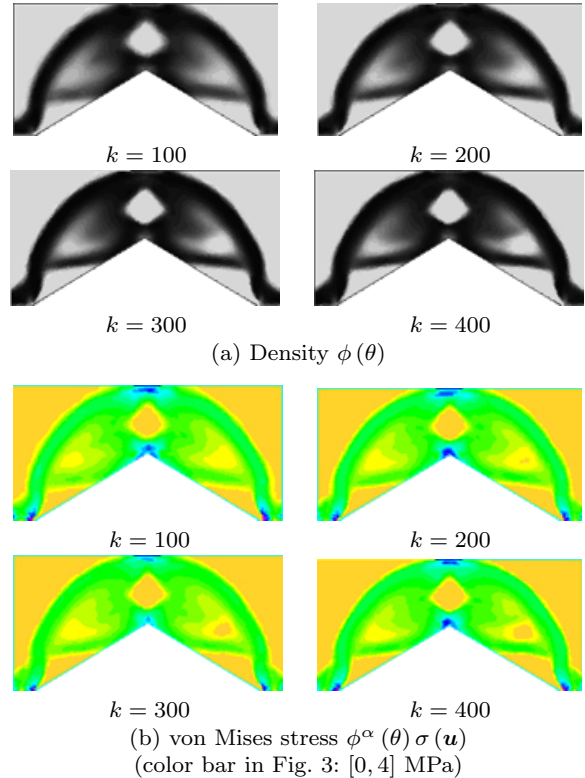


Fig. 16 Portal frame: Results of the H^1 Newton method.

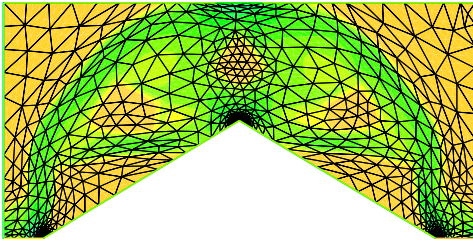


Fig. 17 Mesh of portal frame: $k = 400$ by the H^1 Newton method.

ogy and shape of their result when the two constraints were used is similar to those of the current result. However, the volume rates are 0.409 and 0.5 in the results of the extant study and the current result respectively, and thus a thin beam in a direction perpendicular to the beams similar to the spokes of a wheel appears in the results of the present study. Regarding the computational cost, our proposed methods are found to be significantly slower than other compared literature.

With respect to the portal frame problem, we refer to a numerical result in Le et al. (2010). They analyzed the optimum density by using the p -norm of von Mises stress as the objective function with the volume constraint. Although the volume rates are 0.3 and 0.5 in the previous study and the current analyses, respectively, we observe the same tendencies wherein the layout of major holes and the state of concentration around the center corner and extension to the horizontal direction of density are similar.

6 Conclusions

In this study, a numerical solution of a topology optimization of linear elastic body for minimizing the maximum von Mises stress was investigated. The topology optimization problem was formulated by using the density that was defined by a sigmoid function of the design variable θ . With respect to the objective cost function, the KS function of von Mises stress was used to overcome the non-differentiability of the maximum von Mises stress in addition to the mean compliance. The volume was used as a constraint function. The θ derivative of the objective cost function was derived by using the solution of the adjoint problem with respect to the KS function. As a result of this study, the second θ derivative that is termed as the θ -Hessian of the KS function was derived by using the second θ derivative of the Lagrange function for the KS function together with the θ derivative of the Lagrange function for the linear elastic problem. The θ -Hessians of the cost functions were used to present a solution based on a H^1 Newton method. The validity of the solution was ver-

ified through numerical examples by using a program developed in FreeFEM++. From the results, in keeping with theoretical expectations, the Newton method displays the property of quadratic convergence and the H^1 Newton method is superior to the H^1 gradient method with respect to the convergence speed. In addition, the improvement rate of convergence speed by the H^1 Newton method when compared to that of the H^1 gradient method was observed to rely on the problem setting of the linear elastic problem.

Acknowledgements This work was supported by JSPS KAKENHI Grant Numbers JP16K05285 and JP17K05140.

Appendix

A Abstract optimum design problem

In this appendix, we summarized the basic theories used in this paper (Azegami, 2017). Here, we define an abstract optimum design problem and show the several results with respect this problem. It is assumed that $\phi \in \mathcal{D} \subset X$ is a design variable from an admissible set \mathcal{D} in a Hilbert space X . For $\phi \in \mathcal{D}$, a state variable u in a Hilbert space U is assumed as uniquely determined as a solution of the following problem.

Problem 7 (Abstract variational problem) For $\phi \in \mathcal{D}$, it is assumed that $a(\phi) : U \times U \rightarrow \mathbb{R}$ is a bounded and coercive bilinear form in U , and $l(\phi) = l(\phi)(\cdot) = \langle l(\phi), \cdot \rangle \in U'$ (dual space of U). Find $u \in U$ such that

$$a(\phi)(u, v) = l(\phi)(v) \quad \forall v \in U.$$

Problem 7 is equivalently stated as follows. “Let $\tau(\phi) : U \rightarrow U'$ correspond to an isomorphism by Lax-Milgram theorem when $a(\phi)(\cdot, \cdot)$ is a bounded and coercive bilinear form in U . Find $u \in U$ that satisfies

$$s(\phi, u) = l(\phi) - \tau(\phi)u = 0_{U'}.” \quad (50)$$

We assume that a solution u of Problem 7 is an element of admissible set $\mathcal{S} \subset U$ to assure that $\phi + \varphi \in \mathcal{D}$ where φ is a variation of the design variable ϕ obtained by the gradient or the Newton method that is subsequently demonstrated. Given the pair $(\phi, u) \in \mathcal{D} \times \mathcal{S}$, we consider the following design problem.

Problem 8 (Abstract optimum design problem)

For $f_0, \dots, f_m : \mathcal{D} \times \mathcal{S} \rightarrow \mathbb{R}$, find $(\phi^*, u^*) \in \mathcal{D} \times \mathcal{S}$ such that

$$f_0(\phi^*, u^*) = \min_{(\phi, u) \in \mathcal{D} \times \mathcal{S}} \{ f_0(\phi, u) \mid f_1(\phi, u) \leq 0, \dots, f_m(\phi, u) \leq 0, \text{ Problem 7} \}.$$

A.1 Gradient of cost function f_i with respect to ϕ

In Problem 8, Problem 7 is assumed as an equality constraint. In this section, using the following problem, we show the computations of the Fréchet derivative and Hessian of the cost function f_i with respect to an arbitrary variation $\varphi \in X$ (or $\varphi \in Y \subset X$ with a linear space $Y \supset \mathcal{D}$) of the design variable $\phi \in \mathcal{D}$ subject to the given equality constraint.

Problem 9 (Abstract problem with constraint)

For $f_i : \mathcal{D} \times \mathcal{S} \rightarrow \mathbb{R}$ and $s(\phi, u)$ in (50), find (ϕ^*, u^*) such that

$$f_i(\phi^*, u^*) = \min_{(\phi, u) \in \mathcal{D} \times \mathcal{S}} \{f_i(\phi, u) \mid s(\phi, u) = 0_{U'}\}.$$

In order to show necessary and sufficient conditions for a local minimizer of Problem 9, we define the Lagrange function with respect to Problem 9 as

$$\mathcal{L}_i(\phi, u, v_i) = f_i(\phi, u) + \langle s(\phi, u), v_i \rangle = f_i(\phi, u) + \mathcal{L}_S(\phi, u, v_i), \quad (51)$$

where $\mathcal{L}_S(\phi, u, v_i)$ denotes the Lagrange function with respect to Problem 7, and u and v_i denote the variables in $\mathcal{S} \subset U$ corresponding to the solution of Problem 7 and the Lagrange multiplier with respect to the equality constraint of Problem 7 for f_i respectively. In the definition of Lagrange function of (51), it should be noted that u is not necessary as the solution of Problem 7. Thus, \mathcal{S} and U are used as the admissible set and the set for test function of u and v_i in Problem 7 and the adjoint problem shown later in (62), respectively. With respect to an arbitrary variation $(\varphi, \hat{u}, \hat{v}_i) \in X \times U^2$ of $(\phi, u, v_i) \in \mathcal{D} \times \mathcal{S}^2$, the Fréchet derivative of \mathcal{L}_i is expressed as

$$\begin{aligned} \mathcal{L}'_i(\phi, u, v_i)[\varphi, \hat{u}, \hat{v}_i] &= \mathcal{L}_{i\phi}(\phi, u, v_i)[\varphi] + \mathcal{L}_{iu}(\phi, u, v_i)[\hat{u}] + \mathcal{L}_{iv_i}(\phi, u, v_i)[\hat{v}_i] \\ &= f'_i(\phi, u)[\varphi, \hat{u}] + \langle s'(\phi, u)[\varphi, \hat{u}], v_i \rangle + \langle s(\phi, u), \hat{v}_i \rangle \\ &= f_{i\phi}(\phi, u)[\varphi] + f_{iu}(\phi, u)[\hat{u}] \\ &\quad + \langle s_\phi(\phi, u)[\varphi] + s_u(\phi, u)[\hat{u}], v_i \rangle + \langle s(\phi, u), \hat{v}_i \rangle \\ &= (\langle f_{i\phi}(\phi, u), \varphi \rangle + \langle s_\phi(\phi, u)[\varphi], v_i \rangle) \\ &\quad + \langle f_{iu}(\phi, u) - \tau^*(\phi)v_i, \hat{u} \rangle + \langle s(\phi, u), \hat{v}_i \rangle \\ &= \langle g_i(\phi, u, v_i), \varphi \rangle + \mathcal{L}_{iu}(\phi, u, v_i)[\hat{u}] + \mathcal{L}_S(\phi, u, \hat{v}_i). \end{aligned} \quad (52)$$

Here, $\tau^*(\phi) : U \rightarrow U'$ denotes the adjoint operator of $\tau(\phi)$. Using the notations in (52), we obtain the following result (Theorem 2.1 in Azegami (2017)).

Theorem 1 (The first-order necessary condition)

Let $f_i \in C^1(\mathcal{D} \times \mathcal{S}; \mathbb{R})$ and $s \in C^1(\mathcal{D} \times \mathcal{S}; U')$. If (ϕ, u) is a local minimizer of Problem 9, there exists a $v_i \in U$ that satisfies

$$\langle g_i(\phi, u, v_i), \varphi \rangle + \mathcal{L}_{iu}(\phi, u, v_i)[\hat{u}] = 0 \quad \forall (\varphi, \hat{u}) \in X \times U, \quad (53)$$

$$\mathcal{L}_S(\phi, u, \hat{v}_i) = 0 \quad \forall \hat{v}_i \in U. \quad (54)$$

Proof From the fact that $s \in C^1(\mathcal{D} \times \mathcal{S}; U')$ and that there exists a unique solution u that satisfies $s(\phi, u) = 0_{U'}$, s satisfies the following assumptions for the implicit function theorem in a neighborhood $B_X \times B_U \subset X \times U$ of $(\phi, u) \in \mathcal{D} \times \mathcal{S}$:

1. $s(\phi, u) = 0_{U'}$,
2. $s \in C^0(B_X \times B_U; U')$,
3. $s(\phi, \cdot) \in C^1(B_U; U')$ with respect to an arbitrary $y = (\phi, w) \in B_X \times B_U$ and $s_u(\phi, u) = -\tau : U \rightarrow U'$ is continuous at (ϕ, u) ,
4. $(s_u(\phi, u))^{-1} = -\tau^{-1} : U' \rightarrow U$ is bounded and linear.

From the implicit function theorem, there exists a neighborhood $\hat{B}_X \times \hat{B}_U \subset B_X \times B_U$ and continuous mapping $v : \hat{B}_X \rightarrow \hat{B}_U$, and $s(\phi, u) = 0_{U'}$ that is expressed as

$$u = v(\phi). \quad (55)$$

Hence, we define $y(\phi) = (\phi, v(\phi)) \in C^1(\mathcal{D}; X \times U)$ and write $f_i(\phi, v(\phi)) = f_i(y(\phi))$ by $\tilde{f}_i(\phi)$. Given that $f_i \in C^1(\mathcal{D} \times \mathcal{S}; \mathbb{R})$, thus the fact that ϕ corresponds to a local minimizer implies that

$$\tilde{f}'_i(\phi)[\varphi] = y'^*(\phi) \circ g_i(\phi, v(\phi))[\varphi] = 0 \quad \forall \varphi \in X. \quad (56)$$

Here,

$$\begin{aligned} g_i(\phi, v(\phi)) &= f'_i(\phi, v(\phi)) \in \mathfrak{L}(X; X' \times U') \\ &= \mathfrak{L}(X; \mathfrak{L}(X \times U; \mathbb{R})), \\ y'(\phi) &\in \mathfrak{L}(X; X \times U), \quad y'^*(\phi) \in \mathfrak{L}(X' \times U'; X'). \end{aligned}$$

In this study, $\mathfrak{L}(X; U)$ denotes the set of all bounded linear operators from X to U and \circ denotes the composition operator. We rewrite (56) as given below. First, we express the admissible set of (ϕ, u) with respect to the equality constraint as

$$S = \{(\phi, u) \in \mathcal{D} \times \mathcal{S} \mid s(\phi, u) = 0_{U'}\}. \quad (57)$$

For $y(\phi) = (\phi, u) \in S$, we denote the kernel of $s'(\phi, u) \in \mathfrak{L}(X \times U; U')$ by

$$T_S(\phi, u) = \{(\varphi, \hat{v}) \in X \times U \mid s'(\phi, u)[\varphi, \hat{v}] = 0_{U'}\} \quad (58)$$

and the space orthogonal to $T_S(\phi, u)$ as

$$T'_S(\phi, u) = \{(\psi, w) \in X' \times U' \mid \langle (\varphi, \hat{v}), (\psi, w) \rangle = 0 \quad \forall (\varphi, \hat{v}) \in T_S(\phi, u)\}.$$

Moreover, the relationship between $T_S(\phi, u)$ and the Fréchet derivative $y'(\phi)[\varphi]$ of $y(\phi) \in S$ with respect to an arbitrary variation $\varphi \in X$ is obtained in the following way. If we take the Fréchet derivative on both sides of $s(\phi, u) = 0_{U'}$ with respect to $\varphi \in X$, then we obtain the following expression

$$s'(\phi, u) \circ y'(\phi)[\varphi] = 0_{U'} \quad \forall \varphi \in X. \quad (59)$$

This relationship shows that the image space $\text{Im } y'(\phi)$ of $y'(\phi)$ actually corresponds to the kernel space $\text{Ker } s'(\phi, u)$ of $s'(\phi, u)$. Therefore, the following relationship is established:

$$T_S(\phi, u) = \text{Im } y'(\phi). \quad (60)$$

We use the fore-mentioned relationship to rewrite (56). When ϕ is a local minimizer, it is necessary for $g(\phi, v(\phi))$ to be orthogonal to an arbitrary $(\varphi, v_i) \in T_S(\phi, u)$. Hence,

$$g_i(\phi, v(\phi)) \in T'_S(\phi, u). \quad (61)$$

Now, the relationship between the orthogonal complement space of the image space and the kernel space is used to obtain $T'_S(\phi, u) = \text{Im } s'^*(\phi, u)$ where $s'^*(\phi, u) \in \mathfrak{L}(U; X' \times U')$ denotes the adjoint of $s'(\phi, u)$. Therefore, (61) indicates that we can determine an element v_i of U such that

$$f'_i(\phi, u)[\varphi, \hat{u}] + \langle s'(\phi, u)[\varphi, \hat{u}], v_i \rangle = 0 \quad \forall (\varphi, \hat{u}) \in X \times U.$$

This established equation (53). Moreover, (54) holds if u is the solution of (50). (QED)

From Theorem 1, g_i is evaluated as follows. It is assumed that u is determined as satisfying (54). This means u is the solution of Problem 7. Furthermore, let v_i be determined through the following equation

$$\mathcal{L}_{iu}(\phi, u, v_i)[\hat{u}] = \langle f_{iu}(\phi, u) - \tau^*(\phi)v_i, \hat{u} \rangle = 0 \quad \forall \hat{u} \in U. \quad (62)$$

The problem involving the determination of v_i by (62) is termed as the adjoint problem of Problem 7 with respect to f_i . When we use the solutions u and v_i , $g_i \in X'$ is obtained as follows:

$$\langle g_i(\phi, u, v_i), \varphi \rangle = \langle f_{i\phi}(\phi, u), \varphi \rangle + \langle s_\phi(\phi, u)[\varphi], v_i \rangle \quad \forall \varphi \in X. \quad (63)$$

A.2 Hessian of cost function f_i with respect to variation of ϕ

Furthermore, when f_i and s denote the second-order Fréchet differentiable, then we calculate the second-order partial Fréchet derivative of \mathcal{L}_i with respect to arbitrary variations $(\varphi_1, \hat{v}_1), (\varphi_2, \hat{v}_2) \in T_S(\phi, u)$ of $(\phi, u) \in S$ as

$$\begin{aligned} & \mathcal{L}_{i(\phi, u)(\phi, u)}(\phi, u, v_i)[(\varphi_1, \hat{v}_1), (\varphi_2, \hat{v}_2)] \\ &= f_i''(\phi, u)[(\varphi_1, \hat{v}_1), (\varphi_2, \hat{v}_2)] \\ &+ \langle s''(\phi, u)[(\varphi_1, \hat{v}_1), (\varphi_2, \hat{v}_2)], v_i \rangle, \end{aligned} \quad (64)$$

where

$$S = \{(\phi, u) \in \mathcal{D} \times \mathcal{S} \mid s(\phi, u) = 0_{U'}\}, \quad (65)$$

$$T_S(\phi, u) = \{(\varphi, \hat{u}) \in X \times U \mid s'(\phi, u)[\varphi, \hat{u}] = 0_{U'}\}. \quad (66)$$

This is used to obtain the following result (Theorem 2.2 in Azegami (2017)).

Theorem 2 (The second-order necessary condition)

Let f_i and s be the elements of $C^2(\mathcal{D} \times \mathcal{S}; \mathbb{R})$ and $C^2(\mathcal{D} \times \mathcal{S}; U')$, respectively. If (ϕ, u) is a local minimizer of Problem 9, the following expression holds:

$$\begin{aligned} & \mathcal{L}_{i(\phi, u)(\phi, u)}(\phi, u, v_i)[(\varphi, \hat{v}), (\varphi, \hat{v})] \geq 0 \\ & \forall (\varphi, \hat{v}) \in T_S(\phi, u). \end{aligned} \quad (67)$$

Proof In the proof of Theorem 1, the assumption for the implicit function theorem is replaced by $s(\phi, \cdot) \in C^2(B_U; U')$, and then $v(\phi)$ is used in (55), $y(\phi) = (\phi, v(\phi)) \in C^2(\mathcal{D}; X \times U)$ is determined. From (59), we obtain the following expression:

$$s''(\phi, u)[y'(\phi)[\varphi], y'(\phi)[\varphi]] = 0_{U'} \quad (68)$$

with respect to $y'(\phi)[\varphi] \in T_S(\phi, u)$. Hence, if (ϕ, u) is a local minimizer of Problem 9,

$$\begin{aligned} & \mathcal{L}_{i(\phi, u), (\phi, u)}(\phi, u, v_i)[y'(\phi)[\varphi], y'(\phi)[\varphi]] \\ &= \tilde{f}_i''(\phi)[\varphi, \varphi] \geq 0 \end{aligned} \quad (69)$$

holds with respect to $y'(\phi)[\varphi] \in T_S(\phi, u)$. (QED)

The left-hand side of (67) is the Hessian of f_i with respect to an arbitrary variation $\varphi \in X$ of ϕ , and thus we express it as $h_i(\phi, u, v_i)[\varphi, \varphi]$, and obtain the following result (Theorem 2.3 in Azegami (2017)).

Theorem 3 (The second-order sufficient condition)

Under the assumptions of Theorem 2, if (53) and (54) are satisfied at $(\phi, u, v_i) \in \mathcal{D} \times \mathcal{S}^2$ and (67) holds, then $(\phi, u) \in X \times U$ is a local minimizer of Problem 9.

Proof When $(\phi, u, v_i) \in \mathcal{D} \times \mathcal{S}^2$ is a stationary point of \mathcal{L}_i in S , with respect to an arbitrary point $y(\phi + \varphi) = y(\phi) + z(\varphi)$ in a neighborhood $B \subset S$ of $y(\phi) = (\phi, u)$, there exists a $\theta \in (0, 1)$ that satisfies

$$\begin{aligned} \tilde{f}_i(\phi + \varphi) - \tilde{f}_i(\phi) &= \frac{1}{2} \mathcal{L}_i''(\phi + \theta\varphi, u, v_i)[z(\varphi), z(\varphi)] \\ & \forall y(\phi) + z(\varphi) \in B. \end{aligned}$$

From the assumption, the right-hand side is greater than or equal to 0, and thus $\tilde{f}_i(\phi) \leq \tilde{f}_i(\phi + \varphi)$ holds. (QED)

In view of Theorem 3, h_i is calculated as

$$\begin{aligned} & h_i(\phi, u, v_i)[\varphi_1, \varphi_2] \\ &= (\mathcal{L}_{i\phi}(\phi, u, v_i)[\varphi_1] + \mathcal{L}_{iu}(\phi, u, v_i)[\hat{v}_1])_\phi[\varphi_2] \\ &+ (\mathcal{L}_{i\phi}(\phi, u, v_i)[\varphi_1] + \mathcal{L}_{iu}(\phi, u, v_i)[\hat{v}_1])_u[\hat{v}_2] \\ &= \mathcal{L}_{i\phi\phi}(\phi, u, v_i)[\varphi_1, \varphi_2] + \mathcal{L}_{iu\phi}(\phi, u, v_i)[\hat{v}_1, \varphi_2] \\ &+ \mathcal{L}_{i\phi u}(\phi, u, v_i)[\varphi_1, \hat{v}_2] + \mathcal{L}_{iuu}(\phi, u, v_i)[\hat{v}_1, \hat{v}_2], \end{aligned} \quad (70)$$

where in order to obtain $(\varphi_j, \hat{v}_j) \in T_S(\phi, u)$ for $j \in \{1, 2\}$, \hat{v}_j is determined by using the following equation

$$\mathcal{L}_{S\phi}(\phi, u, v)[\varphi_j] + \mathcal{L}_{Su}(\phi, u, v)[\hat{v}_j] = 0 \quad \forall \varphi_j \in X. \quad (71)$$

B Regularity of H^1 Gradient Method

With respect to the weak solutions of the H^1 gradient method (Problem 4) of θ type, the following result is obtained (Azegami, 2016, Theorem 8.5.5). Here, we assume that g_i are contained in $L^{q_R}(D; \mathbb{R})$ ($q_R > d$). In reality, when $\mathbf{u} \in \mathcal{S}$, g_0 in (19) is contained in $L^{q_R}(D; \mathbb{R})$. Furthermore, the neighborhoods of the singular points are denoted as B as follows: when D is a two-dimensional domain, concave corner points on ∂D and corner points on $\partial\Gamma_D$ in mixed boundary conditions in which the opening angle exceeds $\pi/2$, and when D is a three-dimensional domain, concave edges on ∂D and edges on $\partial\Gamma_D$ in mixed boundary conditions in which the opening angle exceeds $\pi/2$. Additionally, $f_i(\theta, \mathbf{u})$ when $\mathbf{u} \in \mathcal{S}$ is the solution to Problem 1 and is expressed as $\tilde{f}_i(\theta)$.

Theorem 4 (H^1 gradient method of θ type) With respect to $g_i \in L^{q_R}(D; \mathbb{R})$, the weak solutions ϑ_{g_0} of Problem 4 exist uniquely. ϑ_{g_i} is $W^{1, \infty}$ class on $D \setminus \bar{B}$. Moreover, ϑ_{g_i} faces the descent direction of $\tilde{f}_i(\theta)$.

Proof From the fact that g_i is in $L^{q_R}(D; \mathbb{R}) \subset X'$, the Lax-Milgram theorem states that the weak solutions ϑ_{g_i} of Problem 4 uniquely exist. Moreover, the following results are obtained with respect to the regularity of the solution ϑ_{g_i} . Given that ϑ_{g_i} satisfies the elliptic partial differential equation, the differentiability increases by two-orders when compared to g_i , and it corresponds to the W^{2, q_R} class on $D \setminus \bar{B}$. If Sobolev's embedding theorem is applied to this, when $q_R > d$,

$$2 - \frac{d}{q_R} = 1 + \sigma > 1$$

holds, where $\sigma \in (0, 1)$. Therefore, in Sobolev's embedding theorem, when $p = q_R$, $q = \infty$, $k = 1$ and $j = 1$,

$$W^{2, q_R}(D \setminus \bar{B}, \mathbb{R}) \subset W^{1, \infty}(D \setminus \bar{B}, \mathbb{R})$$

holds on $D \setminus \bar{B}$. Here, ϑ_{g_i} corresponds to $W^{1,\infty}$ class on $D \setminus \bar{B}$. Furthermore,

$$\begin{aligned} \tilde{f}_i(\theta + \bar{\epsilon}\vartheta_{g_i}) - \tilde{f}_i(\theta) &= \bar{\epsilon}\langle g_i, \vartheta_{g_i} \rangle + o(|\bar{\epsilon}|) \\ &= -\bar{\epsilon}a_X(\vartheta_{g_i}, \vartheta_{g_i}) + o(|\bar{\epsilon}|) \leq -\bar{\epsilon}\alpha_X \|\vartheta_{g_i}\|_X^2 + o(|\bar{\epsilon}|) \end{aligned}$$

holds with respect to a positive constant $\bar{\epsilon}$. Here, if $\bar{\epsilon}$ is considered as sufficiently small, $\tilde{f}_i(\theta)$ decreases. (QED)

C FreeFEM++ code

```
string caption;//Variable for caption
int k;//Iteration number
int kN=7;//Iteration no. starting H1 Newton method
int kmax=400;//Upper limit of iteration number
real errelas=0.05;//Error level for mesh adaptation
real f0;//f_0
real f0init;//Initial f_0
real flimit;//Initial f_1+c_1
real f1;//f_1+c_1
real product0;//<g_1, vartheta_g0>
real product1;//<g_1, vartheta_i_g0>
real lambda;//Lagrange multiplier
real f0err=0.0001;//Terminal condition
real ca=0.5;//c_a in Eq. (43)
real cd=0.7;//c_D in Eq. (35)
real vonmaximum;//Maximum sigma
real p=50.;//p in Eq. (7)
real sigmabar=140.;//bar_sigma in Eq. (7)
real alpha=3.;//alpha in Problem 1
real ey=210.;//Young's modulus
real nu=0.3;//Poisson's ratio
real l=ey*nu/((1+nu)*(1-2*nu));//Lame constant
real mu= ey/(2*(1+nu));//Lame constant
real area=1;
macro tau(u) ((dx(u#2)+dy(u#1))/2)//
macro E(u) [dx(u#1),tau(u),tau(u),dy(u#2)]//
macro div(u) (dx(u#1)+dy(u#2))//
macro S11(u) (1*div(u)+2*mu*dx(u#1))//
macro S22(u) (1*div(u)+2*mu*dy(u#2))//
macro S12(u) (2*mu*tau(u))//
macro S21(u) (2*mu*tau(u))//
macro S(u) [S11(u),S12(u),S21(u),S22(u)]//
macro von(u) sqrt(((3*(mu^2)*((dy(u#1)+dx(u#2))^2)
+((dy(u#2)*1+dx(u#1)*(1+2*mu))^2)-((dy(u#2)*1
+dx(u#1)*(1+2*mu))*(dx(u#1)*1+dy(u#2)*(1+2*mu)))
+((dx(u#1)*1+dy(u#2)*(1+2*mu))^2)))/Eq. (6)
macro ax(V,f) (ca*(dx(V)*dx(f)+dy(V)*dy(f)+cd*V*f)
//Eq. (35)

int Dirichlet=1;
int Free=2;
int Neumann= 3;
border a1(t=-4,-0.99){x=20;y=t;label=Free;};
border a2(t=-0.99,1.01){x=20;y=t;label=Neumann;};
border a3(t=1.01,4){x=20;y=t;label=Free;};
border c(t=16,-4){x=0;y=t;label=Free;};
border b(t=1,0){x=-20*t+20;y=-4;label=Free;};
border d(t=0,0.6){x=-20*t+20;y=4;label=Free;};
border e(t=0,12){x=8;y= 4+t;label=Free;};
border f(t=0,0.4){x=8-20*t;y=16;label=Dirichlet;};

mesh Th= buildmesh(b(100)+a1(15)+a2(2)+a3(15)
+d(60)+e(60)+f(40)+c(100));
fespace Xh(Th,P2);//Function space for theta type
```

```
fespace Vh2(Th,[P2,P2]);//Function space for u type
Vh2 [u1,u2],[v1,v2]);//Function space for Problem 1
Vh2 [w1,w2],[q1,q2]);//Function space for Problem 3
Vh2 [p1,p2]=[0,-1.];;//Function space for p_N
Xh V,V0,V1,Vf;//Function space for Problems 4 and 6
Xh theta=0.0;//Initial theta
Xh phiplot;//phi for plot
Xh vonMisesplot;//sigma for plot
Xh vonMises=sqrt(((3*(mu^2)*((dy(u1)+dx(u2))^2)
+((dy(u2)*1+dx(u1)*(1+2*mu))^2)-((dy(u2)*1
+dx(u1)*(1+2*mu))*(dx(u1)*1+dy(u2)*(1+2*mu)))
+((dx(u1)*1+dy(u2)*(1+2*mu))^2)))/Eq. (6)
func phi=0.5*tanh(theta)+0.5;//Eq. (1)
func dphi= 0.5/(cosh(theta))^2.;//Eq. (20)
func ddphi=-sinh(theta)/(cosh(theta))^3.;//Eq. (33)
problem elasticity([u1,u2],[v1,v2],solver=UMFPACK)
=int2d(Th)(-phi^alpha*(S(u)'*E(v)))
+int1d(Th,Neumann)(p1*v1+p2*v2)
+on(Dirichlet,u1=0,u2=0);//Problem 1
problem adjointf0([w1,w2],[q1,q2],solver=UMFPACK)
=int2d(Th)((exp(p*phi^alpha*(von(u)/sigmabar))
*phi^alpha)*(((1^2)+(2*mu*1)+(4*(mu^2)))
*(dx(u1)*dx(q1)+dy(u2)*dy(q2)))+((1^2)+(2*mu*1)
-(2*(mu^2)))*(dx(u1)*dy(q2)+dy(u2)*dx(q1)))
+(3*(mu^2)*(dy(u1)+dx(u2))*(dy(q1)+dx(q2))))
*(1/(von(u)*sigmabar)))/int2d(Th)
(exp(p*phi^alpha*(von(u)/sigmabar))))
+int2d(Th)(-phi^alpha*(S(w)'*E(q)))
+int1d(Th,Neumann)(p1*q1+p2*q2)
+on(Dirichlet,w1=0,w2=0);//Problem 3
macro integrandf0(u) (exp(p*phi^alpha*(sqrt(
(3*(mu^2)*((dy(u#1)+dx(u#2))^2)
+((dy(u#2)*1+dx(u#1)*(1+2*mu))^2)
-((dy(u#2)*1+dx(u#1)*(1+2*mu))
*(dx(u#1)*1+dy(u#2)*(1+2*mu)))
+((dx(u#1)*1+dy(u#2)*(1+2*mu))^2)/sigmabar)))/f_0
macro compliancef0(u) (p#1*u#1+p#2*u#2)/f_0
macro g0(u,w,V) (exp(p*phi^alpha*(von(u)/sigmabar))
*alpha*phi^(alpha-1)*dphi*(von(u)/sigmabar)*V
/int2d(Th)(exp(p*phi^alpha*(von(u)/sigmabar))
+((-alpha*phi^(alpha-1)*dphi*(S(u)'*E(w))))*V
//g_0 in Eq. (17)
macro g1(V) (dphi*V)//g_1 in Eq. (19)
macro H(u,w,V,f) (((alpha*(alpha-1)*phi^(alpha-2)
*dphi^2+alpha*phi^(alpha-1)*ddphi)*((von(u)/sigmabar)
-(S(u)'*E(w))))+(((2*(alpha*phi^(alpha-1)
*dphi)^2)/(phi^alpha))*((S(u)'*E(w))
-((1/(int2d(Th)(exp(p*phi^alpha*(von(u)/sigmabar))))
*(exp(p*phi^alpha*(von(u)/sigmabar)))*(((1^2)
+(2*mu*1)+(4*(mu^2)))*(dx(u1)*dx(u1)+dy(u2)*dy(u2)))
+(((1^2)+(2*mu*1)-(2*(mu^2)))*(dx(u1)*dy(u2)
+dy(u2)*dx(u1)))+(3*(mu^2)*(dy(u1)
+dx(u2))*(dy(u1)+dx(u2))))
*(1/(von(u)*sigmabar))))))
+lambda*ddphi)*V*f//h_0 in Eq. (30)
problem H1gradientf0(V0,Vf)=int2d(Th)(ax(V0,Vf))
+int2d(Th)(g0(u,w,Vf));//Eq. (34) for f_0
problem H1gradientf1(V1,Vf)=int2d(Th)(ax(V1,Vf))
+int2d(Th)(g1(Vf));//Eq. (34) for f_1
problem H1Newtonf0(V0,Vf)=int2d(Th)(H(u,w,V0,Vf))
+int2d(Th)(ax(V0,Vf))+int2d(Th)(g0(u,w,Vf));//Eq. (45)
problem H1Newtonf1(V1,Vf)=int2d(Th)(H(u,w,V1,Vf))
+int2d(Th)(ax(V1,Vf))+int2d(Th)(g1(Vf));//Eq. (45)

/**Algorithm 2***/
Th=adaptmesh(Th,theta,err=errelas);//
```

```

[theta]=[theta];
f1init=int2d(Th)(phi);//Eq. (8)
f1=f1init;//
elasticity;//Problem 1
adjointf0;//Problem 3
f0init=(1/p)*log(int2d(Th)(integrandf0(u))
/int2d(Th)(area))
+(int1d(Th,Neumann)(compliancef0(u)));//f_0
f0=f0init;
vonMisesplot=phi^alpha*vonMises;
vonmaximum=vonMisesplot[] .max;
mesh Thprec=Th;
cout<<"Initial f_1="<<f1init<<endl;
cout<<"Initial sigma_max = "<<vonmaximum<<endl;
caption="Initial f_0: "+f0+", f_1+c_1: "+f1init;
phiplot=phi;
plot(phiplot,ps="density0.eps",cmm=caption,
fill=1,value=1,greyscale=1);
/* plot(vonMisesplot,ps="vonMises0.eps"
,cmm=caption,fill=1); for phi^alpha*sigma */

for(k=1;k<kN;k=k+1){
cout<<"Iteration "<<k<<" -----"<<endl;
f0init=f0;
H1gradientf0;//Problem 4 for f_0
H1gradientf1;//Problem 4 for f_1
product0=int2d(Th)(g1(V0))//<g_1, vartheta_g0>
product1=int2d(Th)(g1(V1))//<g_1, vartheta_g1>
lambda=-(f1-f1init+product0)/product1;
V=V0+lambda*V1;//vartheta_g in Eq.(42)
theta=theta+V;//
Th=adaptmesh(Th,theta,err=errelas);
[theta]=[theta];
f1=int2d(Th)(phi)//f_1+c_1
elasticity;//Problem 1
adjointf0;//Problem 3
f0=(1/p)*log(int2d(Th)(integrandf0(u))
/int2d(Th)(area))
+(int1d(Th,Neumann)(compliancef0(u)));//f_0
vonMisesplot=phi^alpha*vonMises;
vonmaximum=vonMisesplot[] .max;
cout<<"f_0="<<f0<<endl;
cout<<"sigma_max = "<<vonmaximum<<endl;
cout<<"error="<<(f0init-f0)/f0init
<<"(error < "<<f0err<<)"<<endl;

if(abs(f0init-f0)/f0init<f0err){break;}

caption="Iteration "+k+", f_0: "+f0
+", f_1+c_1: "+f1;
phiplot=phi;
plot(phiplot,ps="density"+k+".eps",
cmm=caption,fill=1,value=1,greyscale=1);
/* plot(vonMisesplot,ps="vonMises"+k+".eps"
,cmm=caption,fill=1); for phi^alpha*sigma */
};

for (k=kN;k<kmax;k=k+1){
cout<<"Iteration "<<k<<" -----"<<endl;
f0init=f0;
H1Newtonf0;//Problem 6 for f_0
H1Newtonf1;//Problem 6 for f_1
product0=int2d(Th)(g1(V0))//<g_1, vartheta_g0>
product1=int2d(Th)(g1(V1))//<g_1, vartheta_g1>
lambda=-(f1-f1init+product0)/product1;
V=V0+lambda*V1;//vartheta_g in Eq.(42)

```

```

theta=theta+V;
Th=adaptmesh(Th,theta,err=errelas);
[theta]=[theta];
f1=int2d(Th)(phi);
elasticity;//Problem 1
adjointf0;//Problem 3
f0=(1/p)*log(int2d(Th)(integrandf0(u))
/int2d(Th)(area))+int1d(Th,Neumann)
(compliancef0(u)));//f_0
vonMisesplot=phi^alpha*vonMises;
vonmaximum=vonMisesplot[] .max;
cout<<"von_maximum="<<vonmaximum<<endl;
cout<<"f_0="<<f0<<endl;
cout<<"error="<<(f0init-f0)/f0init
<<"(error < "<<f0err<<)"<<endl;

if(abs(f0init-f0)/f0init<f0err){break;}

caption="Iteration "+k+", f_0: "+f0
+", f_1+c_1: "+f1;
phiplot=phi;
plot(phiplot,ps="/density"+k+".eps",
cmm=caption,fill=1,value=1,greyscale=1);
/* plot(vonMisesplot,ps="vonMises"+k+".eps"
,cmm=caption,fill=1); for phi^alpha*sigma */
};

caption="Final,Iteration "+k+", f_0: "+f0
+", f_1+c_1: "+f1;
plot(phiplot,ps="/density"+k+".eps",
cmm=caption,fill=1,value=1,greyscale=1);
/* plot(vonMisesplot,ps="vonMises"+k+".eps"
,cmm=caption,fill=1); for phi^alpha*sigma */

```

References

- Allaire G, Caccès E, Vié JL (2016) Second-order shape derivatives along normal trajectories, governed by Hamilton-Jacobi equations. *Struct Multidiscip Optim* 54:1245–1266
- Azegami H (2016) *Shape Optimization Problems* (in Japanese). Morikita Publishing, Tokyo
- Azegami H (2017) Second derivatives of cost functions and H^1 Newton method in shape optimization problems. In: Kimura M, Notsu H, van Meurs P (eds) *Mathematical Analysis of Continuum Mechanics and Industrial Applications II*, Proceedings of the International Conference CoM-FoS16, Springer Singapore, Mathematics for Industry, pp 61–72
- Azegami H, Kaizu S, Takeuchi K (2011) Regular solution to topology optimization problems of continua. *JSIAM Letters* 3:1–4
- Bendsøe MP (1995) *Optimization of Structural Topology, Shape, and Material*. Springer-Verlag, Berlin
- Bourdin B (2001) Filters in topology optimization. *Internat J Numer Methods Engrg* 50(9):2143–2158
- Bruggi M, Duysinx P (2012) Topology optimization for minimum weight with compliance and stress constraints. *Struct Multidiscip Optim* 46:369–384
- Cheng GD, Guo X (1997) ϵ -relaxed approach in structural topology optimization. *Struct Optim* 13:258–266
- Diaz AR, Sigmund O (1995) Checkerboard patterns in layout optimization. *Struct Optim* 10:40–45
- Duysinx P, Bendsøe MP (1998) Topology optimization of continuum structures with local stress constraints. *Internat J Numer Methods Engrg* 43(8):1453–1478

- Guest JK, Prévost JH, Belytschko T (2004) Achieving minimum length scale in topology optimization using nodal design variables and projection functions. *Internat J Numer Methods Engrg* 61(2):238–254
- Hecht F (2012) New development in freefem++. *J Numer Math* 20(3-4):251–265
- Holmberg E, Torstenfelt B, Klarbring A (2013) Stress constrained topology optimization. *Struct Multidiscip Optim* 48:33–47
- Kawamoto A, Matsumori T, Yamasaki S, Nomura T, Kondoh T, Nishiwaki S (2011) Heaviside projection based topology optimization by a PDE-filtered scalar function. *Struct Multidiscip Optim* 44:19–24
- Kreisselmeier G, Steinhauser R (1979) Systematic control design by optimizing a vector performance index. In: *International Federation of Active Controls Symposium on Computer-Aided Design of Control Systems, Zurich, Switzerland*, pp 29–31
- Kreisselmeier G, Steinhauser R (1983) Application of vector performance optimization to a robust control design for a fighter aircraft. *Internat J Control* 37:251–284
- Lazarov BS, Sigmund O (2011) Filters in topology optimization based on Helmholtz-type differential equations. *Internat J Numer Methods Engrg* 86(6):765–781
- Le C, Norato J, Bruns T, Ha C, Tortorelli D (2010) Stress-based topology optimization for continua. *Struct Multidisc Optim* 41:605–620
- Liu Y, Shimoda M, Shibusaki Y (2015) Parameter-free method for the shape optimization of stiffeners on thin-walled structures to minimize stress concentration. *Journal of Mechanical Science and Technology* 29(4):1383–1390
- París J, Navarrina F, Colominas I, Castelleiro M (2010) Stress constraints sensitivity analysis in structural topology optimization. *Comput Methods Appl Mech Engrg* 199(33-36):2110–2122
- Rozvany G, Zhou M, Birker T (1992) Generalized shape optimization without homogenization. *Struct Optim* 4:250–254
- Shimoda M, Azegami H, Sakurai T (1998) Numerical solution for min-max problems in shape optimization: Minimum design of maximum stress and displacement. *JSME International Journal Series A* 41(1):1–9
- Shintani K, Azegami H (2013) Construction method of the cost function for the minimax shape optimization problem. *JSIAM Letters* 5:61–64
- Sigmund O, Maute K (2013) Topology optimization approaches: A comparative review. *Struct Multidisc Optim* 48:1031–1055
- Sigmund O, Petersson J (1998) Numerical instabilities in topology optimization: A survey on procedures dealing with checkerboards, mesh-dependencies and local minima. *Struct Optim* 16:68–75
- Wang MY, Li L (2013) Shape equilibrium constraint: A strategy for stressconstrained structural topology optimization. *Struct Multidiscip Optim* 47:335–352
- Yang RJ, Chen CJ (1996) Stress-based topology optimization. *Struct Optim* 12:98–105
- Zhang WS, Guo X, Wang MY, Wei P (2013) Optimal topology design of continuum structures with stress concentration alleviation via level set method. *Internat J Numer Methods Engrg* 93(9):942–959